Bioorganic & Medicinal Chemistry xxx (2016) xxx–xxx

Contents lists available at ScienceDirect

Bioorganic & Medicinal Chemistry

journal homepage: www.elsevier.com/locate/bmc

Design, synthesis, and evaluation of 2-piperidone derivatives for the inhibition of β-amyloid aggregation and inflammation mediated neurotoxicity

Lei Li, Ming Chen, Feng-Chao Jiang *

Department of Medicinal Chemistry, Tongji Medical College, Huazhong University of Science and Technology, Wuhan, Hubei 430030, China

ARTICLE INFO

Article history:
Received 4 December 2015
Revised 3 March 2016
Accepted 4 March 2016
Available online xxxx

Keywords:
Alzheimer's disease
2-Piperidone derivatives
β-Amyloid aggregation
Neuroinflammation
Molecular docking
Neuroprotection

ABSTRACT

A series of novel multipotent 2-piperidone derivatives were designed, synthesized and biologically evaluated as chemical agents for the treatment of Alzheimer's disease (AD). The results showed that most of the target compounds displayed significant potency to inhibit $A\beta_{1-42}$ self-aggregation. Among them, compound **7q** exhibited the best inhibition of $A\beta_{1-42}$ self-aggregation (59.11% at 20 μM) in a concentration-dependent manner. Additionally, the compounds **6b**, **7p** and **7q** as representatives were found to present anti-inflammation properties in lipopolysaccharide (LPS)-induced microglial BV-2 cells. They could effectively suppress the production of pro-inflammatory cytokines such as TNF-α, IL-1β and IL-6. Meanwhile, compound **7q** could prevent the neuronal cell SH-SY5Y death by LPS-stimulated microglia cell activation mediated neurotoxicity. The molecular modeling studies demonstrated that compounds matched the pharmacophore well and had good predicted physicochemical properties and estimated IC_{50} values. Moreover, compound **7q** exerted a good binding to the active site of myeloid differentiation factor 88 (MyD88) through the docking analysis and could interfere with its homodimerization or heterodimerization. Consequently, these compounds emerged as promising candidates for further development of novel multifunctional agents for AD treatment.

1. Introduction

Alzheimer's disease (AD) is a progressive multifaceted neurodegenerative disorder that affects millions of elderly people accompanied with cognitive impairment, memory loss, abnormal behavior and decline in language skills.[1] The pathologic hallmarks of AD are the presence of senile plaques (SPs) and neurofibrillary tangles (NFTs) in the brain.[2,3] Although the precise etiology remain elusive, several factors, such as deposits of β-amyloid peptide (Aβ), low levels of acetylcholine (ACh), oxidative stress, inflammation and tau protein hyperphosphorylation play vital roles in the pathogenesis of AD.[4] Moreover, several hypothesis based on the above factors have been suggested to make clear the mechanism of AD pathogenesis.[5]

At present, the hypothesis to explain the mechanism of AD development contain the classic 'amyloid hypothesis', conventional 'cholinergic hypothesis' and 'inflammatory hypothesis', etc.[6–8] According to the 'cholinergic hypothesis', the recession of ACh level leads to cognitive and memory deficits. So, maintaining and recovering the cholinergic function is deemed to be beneficial to the disease.[9,10] Based on 'amyloid hypothesis', the accumulation of Aβ plaques in the central nervous system (CNS) plays a pivotal role in the pathology of AD.[11] Aβ peptides include two main abundant isoforms, $A\beta_{1-42}$ and $A\beta_{1-40}$. They are accumulated through sequential cleaving of the amyloid precursor protein (APP) by β- and γ-secretase.[12] Of the two forms of Aβ, $A\beta_{1-42}$ exerts lower solubility and more toxic and has a higher propensity to form fibrillar aggregates. $A\beta_{1-42}$ soluble oligomers and the assembly of its aggregates into fibrils cause strong neuronal toxicity. Therefore, finding compounds that ubiquitously slow or block the process of $A\beta_{1-42}$ aggregation attracts much current attention.[13]

Converging lines of evidences supports the verdict that neuroinflammation is associated with AD pathology.[14–16] The major players involved in the inflammatory process in AD are thought to be the microglia.[17] Microglia, the immune cells of the CNS, plays crucial roles in defense against injury and tissue repair.[18,19] There exist a variety of transmembrane pattern-recognition receptors called Toll-like receptors (TLRs) expressed limited to microglia, astrocytes and in the brain. TLRs are a family of innate immune system receptors that respond to pathogen-derived and tissue damage-related ligands.[20] Recent findings indicate that TLRs/

* Corresponding author. Tel./fax: +86 27 83692749.
E-mail address: fengchao@mails.tjmu.edu.cn (F.-C. Jiang).

http://dx.doi.org/10.1016/j.bmc.2016.03.010
0968-0896/

MyD88 signaling pathway is implicated in the pathogenesis of AD. In the CNS, microglia express several different TLRs that, when activate by corresponding pathogen-associated molecular patterns (PAMPs), induce the production of pro-inflammatory cytokines including TNF-α, IL-1β and IL-6, which may increase neuronal damage and results in neuronal cell death in the brain.[21,22] Many literatures also demonstrated that excess $A\beta_{1-42}$ could trigger the inflammatory process in AD, gain the production of pro-inflammatory cytokines through the activation of TLRs/MyD88 signaling pathway, vice versa.[23,24]

The complex nature of AD indicates that a unitary mechanism of action is unable to provide a comprehensive therapeutic approach to such multifaceted neurodegenerative disease. Thus, the efficient therapy is more likely to base on the 'one molecule, multiple targets' paradigm.[25] This strategy is based on the evidence that a compound able to bind to different targets involved in the disease might be more suitable for the treatment.[26–28] So, the designed molecules posses the following properties, like inhibition of self-mediated $A\beta_{1-42}$ aggregation, reduction of the amount of pro-inflammatory factors and prevention of inflammation mediated toxicity, emerged as promising agent for AD treatment. The Liver X Receptor agonist (T0901317) could alleviate AD pathology by acting on amyloid deposition and brain inflammation.[29] Additionally, Schmued LC group reported that the compound K114 could inhibit $A\beta_{1-42}$ aggregation and inflammation in vitro and in vivo in AD/Tg mice.[30]

ST2825 (structure showed in Fig. 1), a peptidomimetic inhibitor of MyD88, could inhibit the homodimerization of MyD88 effectively, and thus block the TLRs/MyD88 signaling pathway. As a result, the nuclear transcription factor κB (NF-κB), a transcription factor downstream of MyD88 signaling pathway that allows production of essential effector molecules like pro-inflammatory cytokines for immune and inflammatory responses, will be suppressed.[31,32] Considering the complex structures and bad thermal stability of **ST2825**, and also its moderate bioactivity due to poor solubility, it is essential to search the non-peptidomimetic compounds with simple structures and owned good stability, as well as preferable solubility. Herein, a series of 2-piperidone derivatives were designed and synthesized. The pharmacological effects of these novel compounds were validated based on the multitarget-directed ligands strategy (MTDLs) by measurement of $A\beta_{1-42}$ self-aggregation inhibitory activities, assessing the ability to regulate the production of pro-inflammatory cytokines (TNF-α, IL-1β and IL-6) stimulated by LPS in microglia and prevent the inflammation mediated toxicity in SH-SY5Y cells. Molecular modeling studies allowed to elucidate the interactions between target compounds and amino acid residues of the active site of MyD88.

2. Results and discussion

2.1. Chemistry

The synthetic strategies to 2-piperidone derivatives (**5a**–**5c**, **6a**–**6b**, **7a**–**7q** and **8**) were illustrated in Scheme 1. Intermediate **2a**–**2d** was synthesized from aromatic aldehydes and malonic acid by Knoevenagel reaction with pyridine as catalyst.[33] Use the *p*-toluenesulfonic acid (TsOH) as promoter to esterify the intermediate **2a**–**2d** with ethanol provided high yields of intermediate **3a**–**3d**.[34] According to described methods, the ethyl 4-nitro-3-phenylbutanoate **4a**–**4d** was synthesized from the intermediate **3a**–**3d** by the Michael addition of nitromethane in quantitative yield.[35]

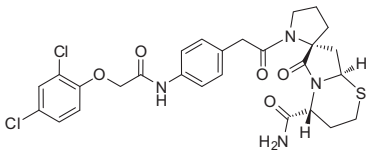

Figure 1. The structure of **ST2825**, a peptidomimetic inhibitor of MyD88.

Compounds **5a**–**5c**, **6a**–**6b**, **7a**–**7q** and **8** were synthesized on the basis of known three-component coupling reactions.[36] The relative stereochemistry of the piperidone core was determined as 4,5-*trans*-5,6-*trans* stereochemistry by NMR analysis as described in the previous paper.[37] A mixture of ethyl 4-nitro-3-phenylbutanoate analogues and *p*-hydroxybenzaldehyde with 3-aminomethylpyridine or methyl 4-(aminomethyl) benzoate were refluxed in ethanol to give the compounds **5a**–**5c** and **6a**–**6b**, respectively. Meanwhile, the intermediate **4a**–**4d** and *p*-hydroxybenzaldehyde were reacted with corresponding substituted benzylamine to furnish the desired compounds **7a**–**7q**. Reaction of the obtained compound **4b** and benzylamine with vanillin produced compound **8**.

2.2. Molecular modeling studies

2.2.1. Pharmacophore mapping

The optimal pharmacophore model was presented in Figure 2. It was consisted of four features, namely, one aromatic ring (AR), one hydrogen bonding acceptor (HBA), two hydrophobic (HYD). According to the 3D crystal structure and the action mechanism of MyD88, we utilized the pharmacophore model to design a series of non-peptidomimetic inhibitors. In order to obey the Lipinski principle,[38] match the pharmacophore model and possess appropriate physical properties, ultimately, twenty-three 2-piperidone derivatives were selected and their activities of MyD88 inhibition were predicted by pharmacophore (Fig. 2).

All the twenty-three compounds were screened through the MyD88 pharmacophore and the whole matched well. As can be seen in Figure 3, the designed compounds (**5b**, **7f**, **7n**, **7o**, **7q**) successfully mapped on all or at least three features of the selected pharmacophore developed against MyD88 as representative. Additionally, the peptidomimetic inhibitor **ST2825** also matched well on all the features of the pharmacophore. The matching values with pharmacophore model and calculated physicochemical properties for designed compounds were shown in Table 1.

2.2.2. Docking analysis

To further study the binding patterns and affinity of the interaction of small molecule with proteins, molecular docking method was performed using software package Ligandfit of Cerius2 (Accelrys Inc.). The protein structure of MyD88 (PDB ID: 4DOM) was obtained from Protein Data bank (PDB) database (shown in Fig. 4A). Structures of individual TIR domains had been determined for a number of receptors and adapters, and most of the TIR domains contained five α helices (A–E) surrounding a central five-stranded β sheet (A–E). Three regions of high sequence conservation were defined as boxes 1–3 motifs and located at the βA strand, BB loop, and αE helix. The residues outside of the BB loop played vital roles for MyD88 dimerization and TLR signaling, such as the CD, DD, and EE loops (Fig. 4A).[39]

Several TIR and TIR domain interaction were observed in the MyD88 in two forms. The former was mediated by αA helix, DD and EE loops from one molecule, interacted with complementary mate αC and αD helices from the other molecule, especially the hydrophobic interactions between F174, Y257, and Y276 with L241 from the other TIR domain. The latter was centered on residues R196 and D197 from the BB loop acted with the complementary mate DD and EE loops of the other TLRs domains by direct or water-mediated hydrogen bonds.

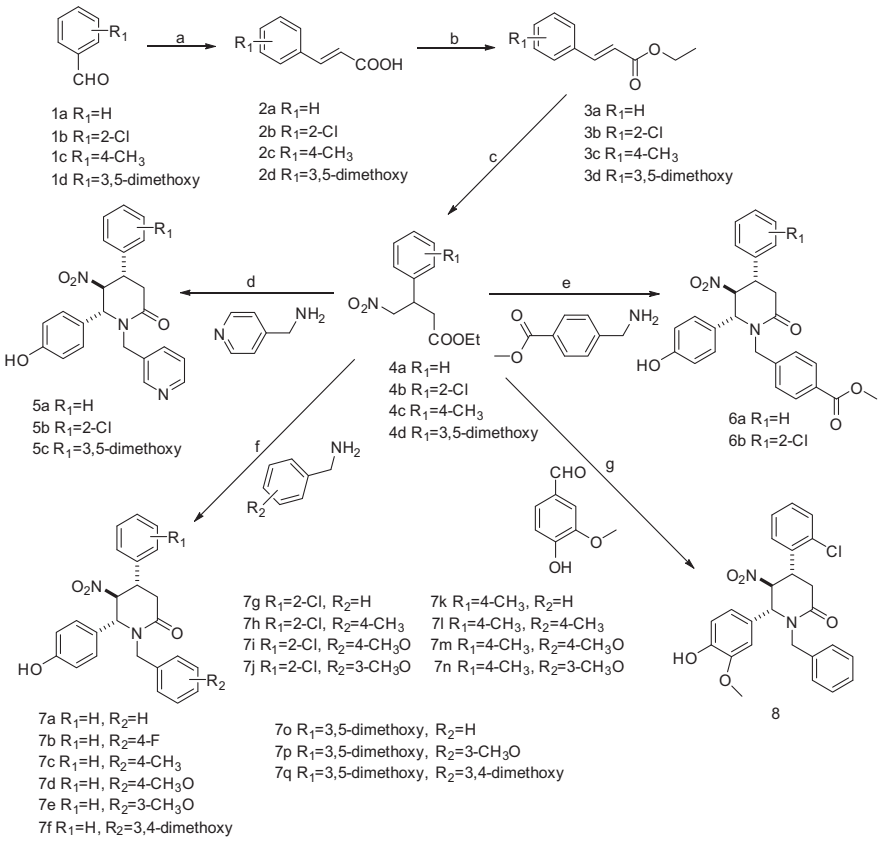

Scheme 1. Synthesis of the 2-piperidone derivatives (**5a–5c**, **6a–6b**, **7a–7q**, **8**). Reagents and conditions: (a) malonic acid, pyridine, piperidine, 90 °C, 2.5 h; (b) ethanol, TsOH, reflux, 12 h; (c) DBU, CH_3NO_2, acetonitrile, 0 °C, 20 h; (d) *p*-hydroxybenzaldehyde, 3-aminomethylpyridine, ethanol, reflux, 24 h. (e) *p*-Hydroxybenzaldehyde, methyl 4-(aminomethyl) benzoate, ethanol, reflux, 24 h. (f) *p*-Hydroxybenzaldehyde, substituted benzylamine, ethanol, reflux, 24 h. (g) Vanillin, benzylamine, ethanol, reflux, 24 h.

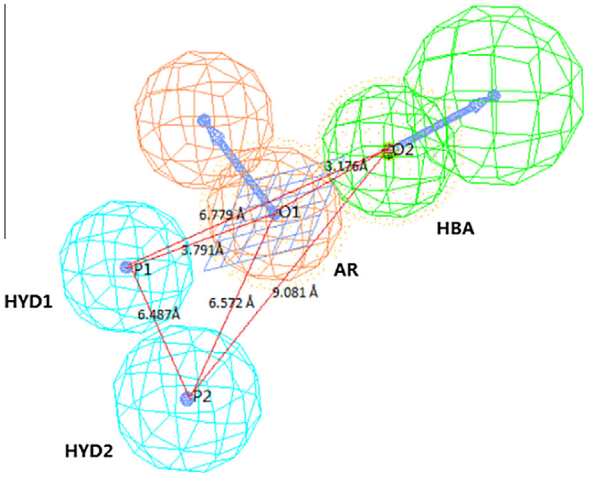

Figure 2. The 3D feature of the optimal pharmacophore model with distance constraints. Two hydrophobic (HYD1 and HYD2), an aromatic ring (AR) and a hydrogen bonding acceptor (HBA) feature of the pharmacophore are color-contoured (HYD, blue; AR, orange; HBA, green).

Herein we used the Ligandfit of Cerius2 (Accelrys Inc.) to dock for MyD88 with compound **7q**. Docking results indicated that the compound **7q** was not directly acted on the residues outside of BB loop (198-VIIWYDEQTLEVGDS-212) of MyD88 to prevent its homodimerization or heterodimerization with other TLRs. Similarly, It was not entered the box 2 or box 1 which related closely to BB loop. Instead, the compound **7q** embed in the box 3 of MyD88 with crooked configuration, and acted on some amino-acid residues of αE, βD, βC, αA, DD loop (260-ILPIWHNINAQEVSKY-275), and EE loop (Fig. 4B).

Here, the benzyl at N-1 position of compound **7q** embed inside of MyD88, acted on L189 of αB, I179 of αA, L191 of βB, A290 of βD, V220 of βC, and L289 of αD by hydrophobic interactions (Fig. 5A). The benzene ring at C-4 position of compound **7q**, located at the surface of Myd88 and combined with K291, A292 and L293 of αE. Additionally, the benzene ring at C-6 position was acted on W286 of DD loop (Fig. 5B).

Although compound **7q** didn't act on the BB loop region directly, it could obviously discern the hydrophobic interactions of the piperidone group with I179 (the active site of BB loop) of αA.[40] As a result, it could weaken the hydrophobic interactions of the I179 with residues L182 and V175, destroy the stability for the basis of the BB loop and change the configuration and the domain interface electron cloud density of BB loop. As we know, the central links of interaction of TIR-TIR were stem from the interaction of BB loop and DD loop of the TLRs domain. All in all, when the compound **7q** embedded in MyD88, it would affect αE, βD, βC, αA, DD loop and EE loop. Simultaneously, the configuration and electron cloud distribution of MyD88 were altered. Furthermore, it could directly impact the interaction of DD loop with BB loop, and also affect the homodimerization or heterodimerization of MyD88 and TIR signaling pathway.

2.3. Inhibition of self-mediated $A\beta_{1-42}$ aggregation

2.3.1. Thioflavin T (ThT) fluorescence assay

The ability of 2-piperidone derivatives to reduce $A\beta_{1-42}$ self-aggregation was evaluated by thioflavin T (ThT) fluorescence

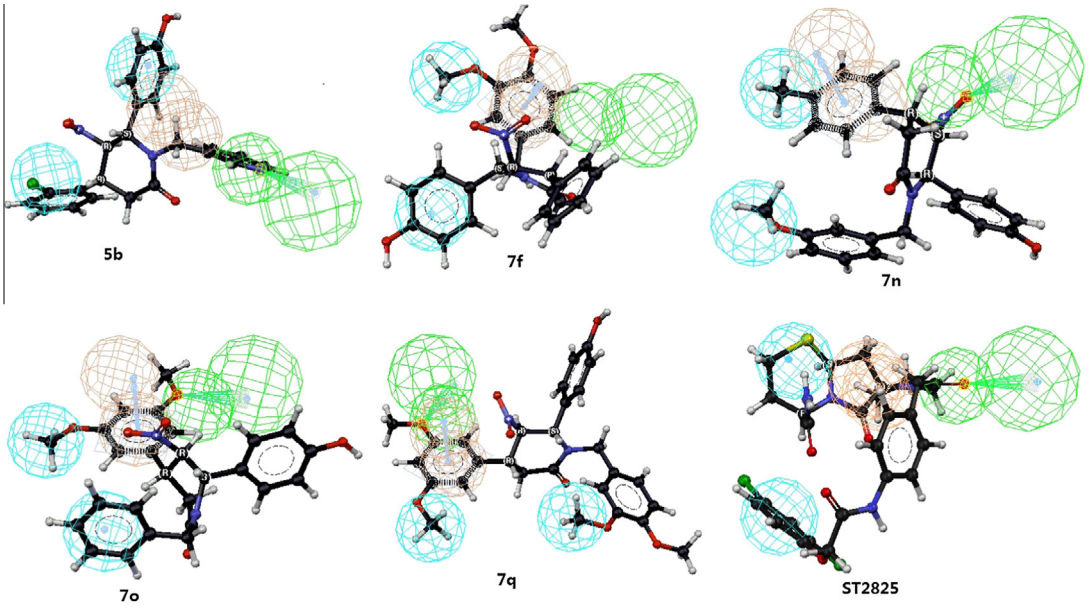

Figure 3. Superimposition of designed compounds and peptidomimetic inhibitor **ST2825** on the optimal pharmacophore developed against MyD88. **5b** (IC_{50} = 5.9 μM), **7f** (IC_{50} = 0.74 μM), **7n** (IC_{50} = 1.4 μM), **7o** (IC_{50} = 0.29 μM), **7q** (IC_{50} = 0.068 μM) and **ST2825** (IC_{50} = 0.67 μM).

Table 1
The matching values with pharmacophore model and calculated physicochemical properties for the designed compounds (**5a**–**5c**, **6a**–**6b**, **7a**–**7q** and **8**)

Compound	IC_{50}[a] (μM)	MW[b]	Log *P*[b]	HBD[b]	HBA[b]
5a	1.2	403.47	2.25	1	7
5b	5.9	437.91	2.91	1	7
5c	0.27	463.53	2.21	1	9
6a	1.4	460.52	3.43	1	8
6b	16	494.96	4.10	1	8
7a	110	402.48	3.43	1	6
7b	8.5	420.47	3.56	1	6
7c	1.5	416.51	3.82	1	6
7d	1.1	432.51	3.29	1	7
7e	1.5	432.51	3.43	1	7
7f	0.74	462.54	3.15	1	8
7g	9.3	436.89	3.88	1	7
7h	1.9	450.95	4.49	1	6
7i	2.6	466.95	3.96	1	7
7j	0.81	466.95	4.09	1	7
7k	1.1	416.51	3.82	1	6
7l	2.5	430.54	4.21	1	6
7m	1.4	446.54	3.68	1	7
7n	1.4	446.54	3.82	1	7
7o	0.29	462.54	3.4	1	8
7p	0.079	492.57	3.39	1	9
7q	0.068	522.6	3.11	1	10
8	0.91	466.95	3.95	1	7

[a] The estimated IC_{50} values were predicted by Catalyst software.
[b] The physicochemical properties were calculated using Pallas 3.3.2.6 software.

assay.[41] Selecting curcumin (Cur), a known active natural product for the inhibition of $A\beta_{1-42}$ self-aggregation, as a reference compound. ThT can selectively localize to amyloid deposits, thereupon display a dramatic increase in fluorescence brightness and intensive fluorescence emission at 490 nm.[42,43] As shown in Table 2 and Figure 6, it could be seen that the bulk of the target compounds should moderate to good potencies (28.73–59.11% at 20 μM) relative to that of curcumin (46.59% at 20 μM), except **7b**, **7g** and **8**. Those three compounds were found to be less pronounced to inhibit $A\beta_{1-42}$ self-aggregation at 20 μM. The compound **8**, with 11.78% inhibitory potency at 20 μM, showed that replacing phenol with guaiacol could not enhance the inhibition potency compared with compound **7g** (11.25% at 20 μM). Moreover, substitutions of the benzyl at N-1 position were examined, changing the benzyl group of compound **7a** to 4-fluorobenzyl (compound **7b**) turned out to be completely inactive (6.39% at 20 μM), however, introduced 3-pyridylmethyl group or methyl 4-methylbenzoate group at the N-1 position retained inhibition activity (**5a**–**5c** or **6a**–**6b**). Remarkably, eight synthesized derivatives (**5b**, **7e**–**7f**, **7j**, and **7n**–**7q**) were more potent than that of reference compound curcumin and can efficiently block $A\beta_{1-42}$ self-aggregation. Among them **5c** (54.01% at 20 μM) and **7o**-**7q** (54.98%, 56.85%, 59.11% at 20 μM, respectively) displayed the highest potency. From the inhibition values of **5c** and **7o**–**7q**, it appeared that 3,5-dimethoxyphenyl at C-4 position played a vital role in determining the inhibition of $A\beta_{1-42}$ self-aggregation. Interestingly, compared with 4-methoxybenzyl at N-1 position (**7d**, **7i**, and **7m**), substituting with 3-methoxybenzyl at N-1 position (**7e**, **7j**, and **7n**) ameliorate the potency of $A\beta_{1-42}$ self-aggregation inhibition.

Additionally, we further evaluated **5a** and **7q** on $A\beta_{1-42}$ aggregation at different concentration. The concentration-effect curves of **5a** and **7q** in Figure 7 showed that they could inhibit $A\beta_{1-42}$ self-aggregation in a concentration-dependent manner.

2.3.2. Atomic force microscopy (AFM) assay

AFM has emerged as a valid tool for distinguishing structures features of the aggregate forms and used to image their morphologies.[44] So, we utilized AFM to be an imaging technique to assess the aggregation process in the presence or absence of the compound **7q**. As can be seen from Figure 8A, in the absence of the compound **7q**, $A\beta_{1-42}$ converted into robust fibrils and large ordered aggregates. In contrast, in the presence of the compound **7q**, no fibrils but some small insoluble globular aggregates were observed (Fig. 8B). It manifested that the difference of the morphologies were mainly contributed to the strong interaction between $A\beta_{1-42}$ aggregates and the compound **7q**. Obviously, the compound **7q** could effectively inhibit $A\beta_{1-42}$ fibrillogenesis. The AFM result of the compound **7q** was in agreement with the above results of ThT assay.

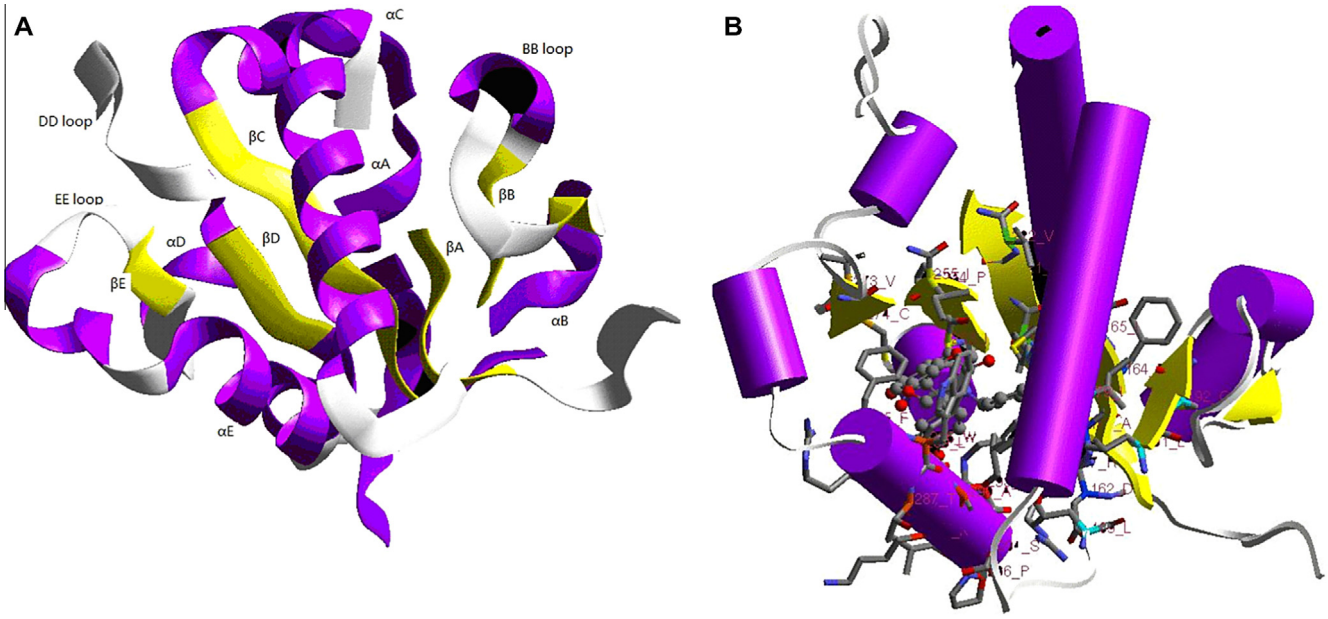

Figure 4. (A) The configuration of MyD88. (B) Compound **7q** enter the box 3 of MyD88 with non-bond interaction (score-1281.682).

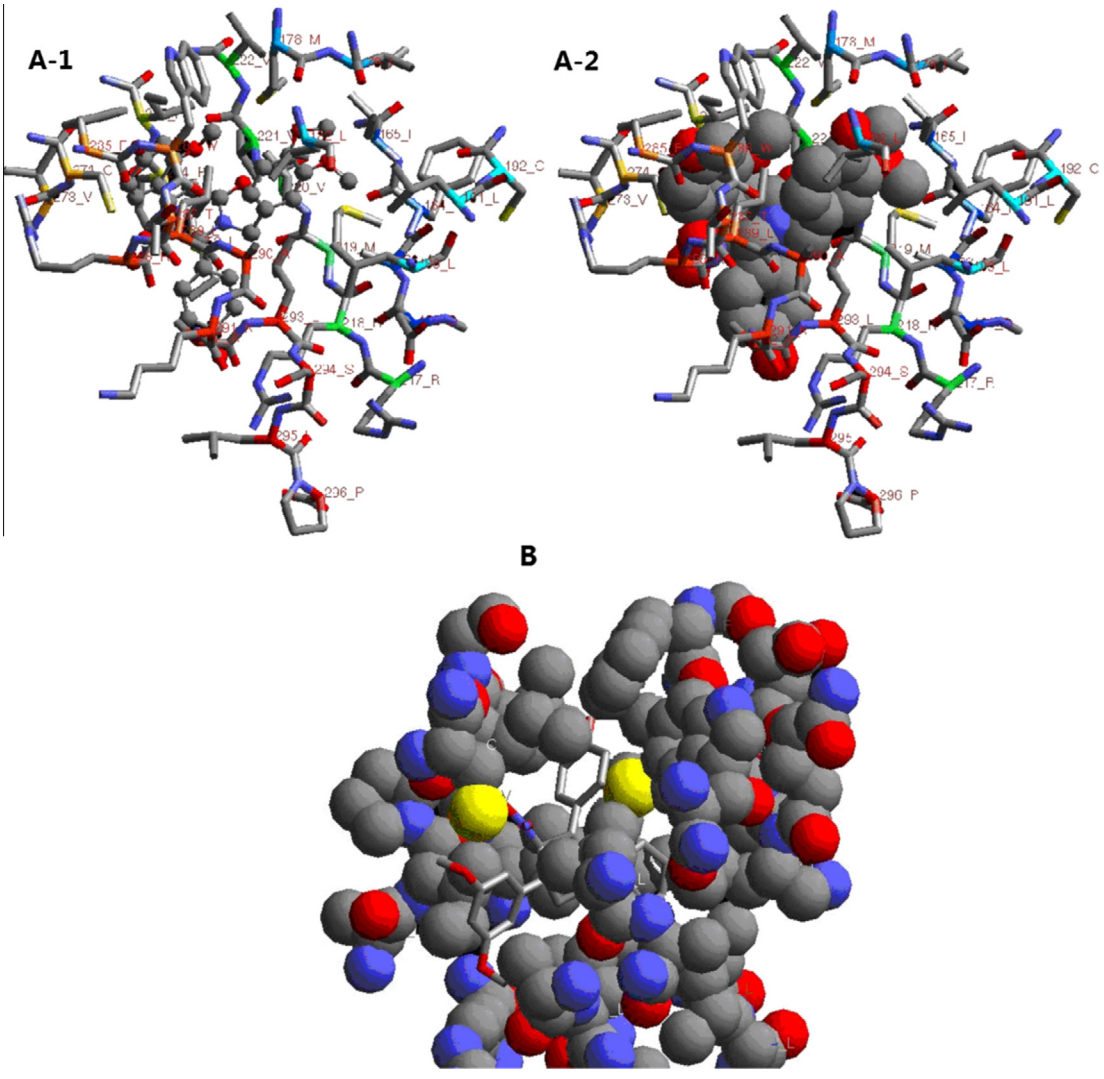

Figure 5. (A) Compound **7q** act with the amino acid residues of MyD88. (B) Compound **7q** embed in MyD88.

Table 2
Inhibition of $A\beta_{1-42}$ self-aggregation by the 2-piperidone derivatives

Compound	$A\beta_{1-42}$ aggregation inhibition[a] (%)	Compound	$A\beta_{1-42}$ aggregation inhibition[a] (%)
5a	43.3 ± 0.6	**7h**	46.1 ± 4.11
5b	41.56 ± 2.23	**7i**	28.73 ± 1.01
5c	54.01 ± 4.33	**7j**	50.03 ± 1.17
6a	36.29 ± 4.45	**7k**	44.1 ± 1.42
6b	33.07 ± 3.53	**7l**	42.06 ± 4.67
7a	43.56 ± 3.5	**7m**	30.6 ± 3.15
7b	6.39 ± 3.52	**7n**	48.85 ± 4.12
7c	39.87 ± 0.8	**7o**	54.98 ± 4.82
7d	46.08 ± 1.63	**7p**	56.85 ± 0.7
7e	51.67 ± 3.17	**7q**	59.11 ± 1.83
7f	49.22 ± 4.13	**8**	11.78 ± 4.6
7g	11.25 ± 2.48	Curcumin	46.59 ± 2.72

[a] Values are expressed as mean ± SD from three independent measurements, each performed in duplicate. Inhibition of $A\beta_{1-42}$ self-aggregation with the tested compounds at concentration of 20 μM.

2.4. Effect of compounds on the production of pro-inflammatory cytokines

We examined the effect of compounds on the production of pro-inflammatory cytokines stimulated by LPS (endotoxin) in microglia such as TNF-α, IL-1β and IL-6. LPS was a validated TLR4 ligand that caused marked activation of microglia both in vitro and in vivo resulted in an increased production of the cytokines.[45] In order to eliminate the interference action induced by the cytotoxic effect of the compound itself, we use the MTT assay to asses the effect on the viability of BV-2 cells of compound **7q** with different concentration. The results manifested that the compound **7q** and LPS at indicated concentration exerted no signs of cytotoxicity (Fig. 9A). Therefore, compounds with the concentration 0.0016, 0.008, 0.04, 0.2 and 1 μmol/L were utilized in the following assay.

We used 1 μg/ml of LPS to induce TNF-α, IL-1β and IL-6 productions in BV-2 microglia. As shown in Figure 9B–D, the pro-inflammatory cytokines TNF-α, IL-1β and IL-6 stimulated by LPS were potently inhibited by the compounds **6b**, **7p** and **7q** in a concentration-dependent manner. Compound **7q** effectively reduced the productions of these three cytokines with an IC_{50} value of 0.08 ± 0.02 μM, 0.21 ± 0.06 μM and 0.03 ± 0.01 μM. Similarly, other two compounds **6b** and **7p** also displayed good potential. Thereinto, **6b** with an IC_{50} value of 0.09 ± 0.02 μM, 3.49 ± 0.12 μM and 0.08 ± 0.01 μM, **7p** with an IC_{50} value of 0.02 ± 0.01 μM, 0.85 ± 0.09 μM and 0.17 ± 0.04 μM, respectively. Therefore compounds **6b**, **7p** and **7q** could effectively inhibit the production of several different pro-inflammatory cytokines stimulated by LPS in microglia. Thus ameliorated the local inflammation atmosphere and regulated the pro-inflammatory cytokines in a rational level.

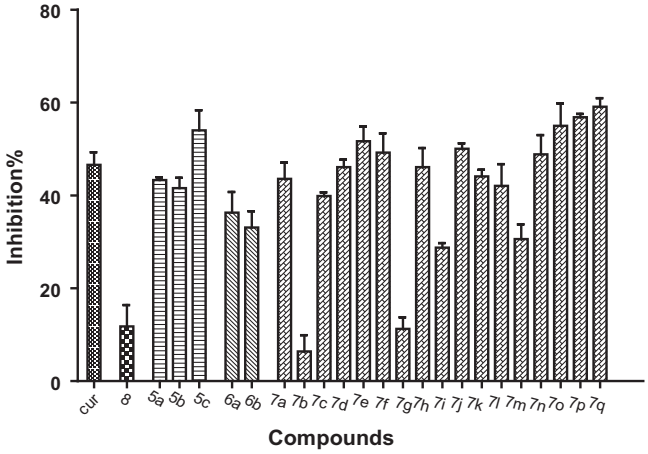

Figure 6. Inhibition of self-mediated $A\beta_{1-42}$ aggregation by 2-piperidone derivatives (**5a**–**5c**, **6a**–**6b**, **7a**–**7q** and **8**) comparing with that of curcumin. The thioflavin T fluorescence assay was used and the mensuration of fluorescence was accomplished in the presence of 20 μM test compound. The mean ± SD values from three independent experiments were shown.

2.5. Prevention of inflammation mediated toxicity in SH-SY5Y cells

Activated microglia, stimulated through LPS, could secrete lots of inflammatory factors that induce apoptotic neuronal cell death. To evaluate the inhibitory potential of compound **7q** on neuronal cell death, compound **7q**-conditioned media (CM) from LPS-stimulated BV-2 cells were applied to SH-SY5Y cells. The MTT assay was used to measure the viability of neuronal cell. As shown in Figure 10B, compound **7q** displayed the moderate effect to prevent neuronal cell death in a concentration-dependent manner. Treatment of SH-SY5Y cells with compound **7q**-conditioned media revealed a significant effect at the dose of 5 μM, with cell viability of 82.92%. Additionally, the compound **7q** under 5 μM exerted no signs of cytotoxicity to SH-SY5Y cells shown in Figure 10A. The neuroprotective results against inflammation mediated toxicity in SH-SY5Y cells showed an excellent correlation with the reduction of several different pro-inflammation cytokines induced by LPS in microglia.

2.6. Co-immunoprecipitation (Co-IP) assay

In order to evaluate and confirm the activity against MyD88 for the designed compounds, Co-IP method was used to study the influence of MyD88 dimerization level with the compound **7q**. As determined by WB analysis, we showed that Flag-MyD88 and HA-MyD88 were successfully co-expressed in HEK293 cells (Fig. 11A). When the Flag-MyD88 and HA-MyD88 were co-expressed in HEK293 cells they could specifically interact and form dimers without the intervention by the compound, as demonstrated by Co-IP experiments (lane 1 in Fig. 11B). Meanwhile, Co-IP with anti-HA antibody and protein A/G agarose-beads indicated that anti-HA antibodies captured Flag-MyD88, which was inhibited by the compound **7q** in a dose-dependent manner (lane 2 and lane 3 in Fig. 11B).

The Co-IP assay support a strong interaction of the compound **7q** with MyD88 directly, compound **7q** could inhibit MyD88 homodimerization in transfected HEK293 cells. Thus the biological results were in agreement with the above docking analysis and confirmed the predicted binding mode.

3. Conclusion

In conclusion, a series of 2-piperidone derivatives were designed, synthesized and biologically evaluated. Most of 2-piperidone

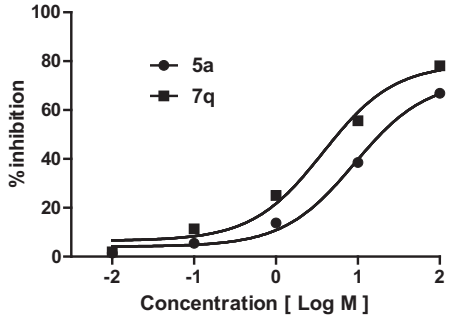

Figure 7. The concentration–effect curves of **5a** (●) and **7q** (■) determined by the ThT assay.

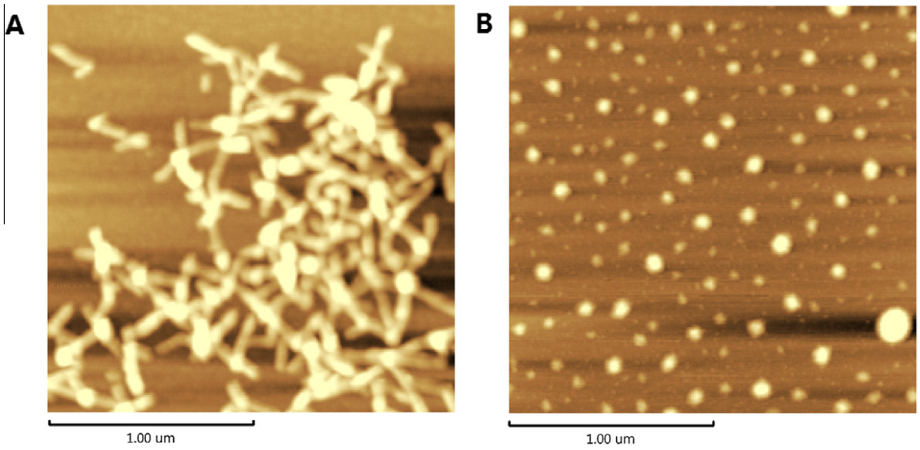

Figure 8. Morphological study of $A\beta_{1-42}$ aggregation by AFM. (A) Aliquots of 25 μM $A\beta_{1-42}$ were incubated alone for 4 days at 30 °C; (B) Aliquots of 25 μM $A\beta_{1-42}$ were incubated in the presence of 50 μM **7q** for 4 days at 30 °C. Scale bars are 1 μm.

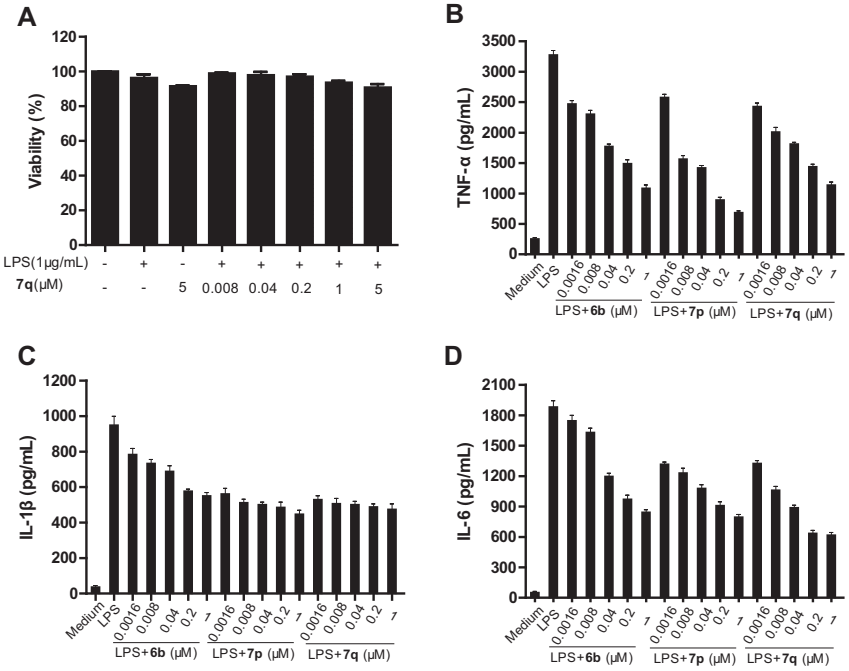

Figure 9. Effect of compounds **5b**, **7p** and **7q** on microglia-mediated cytokine productions. BV-2 cells were pretreated with compound for 3 h and then stimulated with LPS (1 μg/ml) for 12 h. The amount of pro-inflammation cytokines was measured by immunoassays. The cell viability was assessed by MTT assay. (A) Effect of compound **7q** on the viability of BV-2 microglia; (B) TNF-α; (C) IL-1β; (D) IL-6. Each bar shows the mean ± SD of three independent experiments.

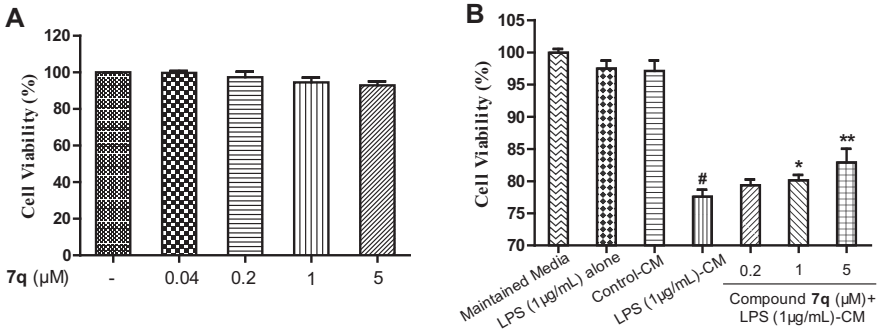

Figure 10. Effect of compound **7q**-conditioned media from LPS-stimulated BV-2 cells on apoptotic neuronal cell death in SH-SY5Y cells. BV-2 microglial cells were pretreated with 0.2, 1 and 5 μM of compound **7q** for 3 h and stimulated with 1 μg/mL of LPS for 12 h. After 12 h LPS treatment, the conditioned media (CM) were collected and treated in SH-SY5Y cells. (A) Effect of compound **7q** on the viability of SH-SY5Y cells; (B) MTT assay. The mean ± SD values from three independent experiments were shown. $^{*}p$ <0.05 and $^{**}p$ <0.001 versus the LPS (1 μg/mL)-CM group, $^{\#}p$ <0.001 versus the control-CM group.

Please cite this article in press as: Li, L.; et al. *Bioorg. Med. Chem.* (2016), http://dx.doi.org/10.1016/j.bmc.2016.03.010

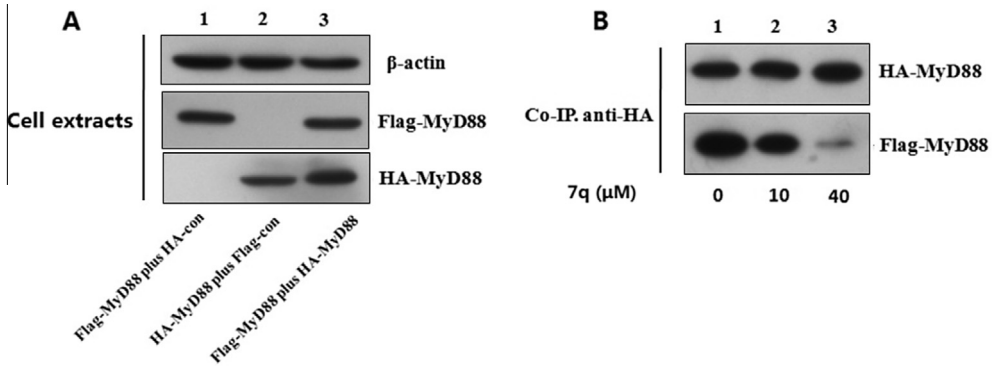

Figure 11. Effect of compound **7q** with the interaction of MyD88. (A) WB analysis of Flag-MyD88 and HA-MyD88 expression in transfected HEK293 cells are shown. HEK293 cells were transfected with Flag-MyD88 alone (lane 1) and HA-MyD88 alone (lane 2) or in combination (lane 3); (B) Dimerization of MyD88 was assessed by Co-IP. Cell lysates were immunoprecipitated with anti-HA, and immunoprecipitated proteins were analyzed by WB using anti-HA or anti-Flag. The inhibit effect of compound **7q** on MyD88 homodimerization is a concentration-dependent.

derivatives showed a good inhibitory potency on $A\beta_{1-42}$ self-aggregation. Especially compound **7q** exhibited the highest inhibitory potency (59.11% at 20 μM), and inhibited $A\beta_{1-42}$ self-aggregation in a concentration-dependent manner. Additionally, compound **7q** could prevent the neuronal cell SH-SY5Y death by LPS-stimulated microglia cell activation mediated neurotoxicity. Moreover, compounds **6b**, **7p** and **7q** effectively suppressed pro-inflammatory cytokines (TNF-α, IL-1β and IL-6) in LPS-activated microglial BV-2 cells. The molecular modeling studies demonstrated that compound **7q** matched the pharmacophore well and obviously discerned the hydrophobic interactions of the piperidone group with the active site of MyD88. Consequently, it could destroy the stability for the basis of the BB loop and change the configuration and the domain interface electron cloud density of MyD88. The demonstration of compound-MyD88 interaction was confirmed by the co-immunoprecipitation assay, compound **7q** could inhibit MyD88 homodimerization in transfected HEK293 cells in a concentration-dependent manner. All in all, such multi-functional properties suggest that these compounds emerged as promising molecules for the therapy of Alzheimer's disease.

4. Experimental section

4.1. Chemistry

Melting points were measured on an uncorrected X-5 Digital melting point apparatus. IR (KBr-disc) spectra were detected by Bruker VERTEX 70 spectrometer one scanning 3500 and 350 cm^{-1}. ^1H NMR and ^{13}C NMR spectra were recorded using TMS as the internal standard in DMSO-d_6 on a Bruker spectrometer at 400 and 100 MHz, respectively. The mass spectra were recorded on a Finnigan LCQ Deca XP™ instrument with an ESI mass selective detector. Reactions were monitored by thin layer chromatography (TLC) on precoated silica gel GF254 (Qingdao Haiyang Chemical Co. Ltd) plates. The purities of all compounds were confirmed by analytical HPLC performed with HITACHI L-2000 instrument and a Diamonsil C18 (2) HPLC column (250 × 4.6 mm, 5 μm), eluted with a gradient of 75% methanol in water at a speed of 1 mL/min. All solvents and reagents were analytical pure and no further purification is needed. All starting materials were commercially available.

4.1.1. General procedure for the preparation of cinnamic acid analogues (2a–2d)

A mixture of malonic acid (12 mmol), aromatic aldehydes (10 mmol), piperidine (15 mmol) and pyridine (0.3 mmol) was stirred at reflux for about 3 h and monitored by TLC. After removal of the solvent under vacuum, the residue was poured into ice water and adjusted PH to 2 with 10% HCl. Then, the precipitate was filtered and washed well with H_2O, recrystallized with 95% alcohol, and dried under vacuum to afford the cinnamic acids analogues **2a**–**2d**.

4.1.1.1. (*E*)-Cinnamic acid (2a). Malonic acid was treated with benzaldehyde according to the general procedure for the synthesis of **2a**–**2d** to obtain the desired product **2a** as white powder in 91.7% yield. Mp 132.9–134.5 °C (lit.[46] 131–133 °C).

4.1.1.2. (*E*)-3-(2-Chlorophenyl)acrylic acid (2b). Malonic acid was treated with 2-chlorobenzaldehyde according to the general procedure for the synthesis of **2a**–**2d** to obtain the desired product **2b** as white powder in 87.5% yield. Mp 210.4–211.5 °C (lit.[47] 210.9–211.2 °C).

4.1.1.3. (*E*)-3-(*p*-Tolyl)acrylic acid (2c). Malonic acid was treated with 4-methylbenzaldehyde according to the general procedure for the synthesis of **2a**–**2d** to obtain the desired product **2c** as white powder in 83.2% yield. Mp 195.9–196.8 °C (lit.[48] 199–200 °C).

4.1.1.4. (*E*)-3-(3,5-Dimethoxyphenyl)acrylic acid (2d). Malonic acid was treated with 3,5-dimethoxybenzaldehyde according to the general procedure for the synthesis of **2a**–**2d** to obtain the desired product **2d** as pale yellow crystalline powder in 85.1% yield. Mp 178.6–180.1 °C (lit.[49] 174–175 °C).

4.1.2. General procedure for the preparation of ethyl cinnamate analogues (3a–3d)

A mixture of cinnamic acid analogue (100 mmol), *p*-toluenesulfonic acid (1.0 g), and anhydrous ethanol (50 mL) was stirred at reflux for about 12 h. After removal of the ethanol under vacuum, the residue was then diluted with water and extracted with diethyl ether. The combined organic phase was washed with 10% sodium bicarbonate solution, dried over anhydrous sodium sulphate, filtered and evaporated.

4.1.2.1. (*E*)-Ethyl cinnamate (3a). Intermediate **2a** was esterified according to the general procedure for the synthesis of **3a**–**3d** to obtain the desired product **3a** as pale yellow oil in 95.1% yield. n_D^{20} 1.5579 (lit.[50] 1.5566).

4.1.2.2. (*E*)-Ethyl 3-(2-chlorophenyl)acrylate (3b). Intermediate **2b** was esterified according to the general procedure for the synthesis of **3a**–**3d** to obtain the desired product **3b** as yellow oil in 88.9% yield. n_D^{20} 1.5443.

4.1.2.3. (*E*)-Ethyl 3-(*p*-tolyl)acrylate (3c). Intermediate **2c** was esterified according to the general procedure for the synthesis of **3a**–**3d** to obtain the desired product **3c** as colorless oil in 80.2% yield. n_D^{20} 1.5616.

4.1.2.4. (*E*)-Ethyl 3-(3,5-dimethoxyphenyl)acrylate (3d). Intermediate **2d** was esterified according to the general procedure for the synthesis of **3a**–**3d** to obtain the desired product **3d** as yellow oil in 79.3% yield. n_D^{20} 1.5483.

4.1.3. General procedure for the preparation of ethyl 4-nitro-3-phenylbutanoate analogues (4a–4d)

A mixture of 1,8-diazabicyclo-[5,4,0]undec-7-ene (DBU) (100 mmol), CH_3NO_2 (200 mmol), and CH_3CN (50 mL) was stirred at a constant low temperature reaction bath. Then the ethyl cinnamate analogue was dropwise added after the temperature was lowered to 0 °C. The reaction was conducted at this temperature for 20 h. The reactants were then poured into water, adjusted PH to 2 with 10% HCl and extracted with ethyl ether. The combined organic phase was washed with water, dried over anhydrous sodium sulphate, filtered and evaporated.

4.1.3.1. Ethyl 4-nitro-3-phenylbutanoate (4a). Intermediate **3a** was treated with nitromethane according to the general procedure for the synthesis of **4a**–**4d** to obtain the desired product **4a** as pale yellow oil in 91.1% yield. n_D^{20} 1.5112.

4.1.3.2. Ethyl 3-(2-chlorophenyl)-4-nitrobutanoate (4b). Intermediate **3b** was treated with nitromethane according to the general procedure for the synthesis of **4a**–**4d** to obtain the desired product **4b** as light brown oil in 91.6% yield. n_D^{20} 1.5325.

4.1.3.3. Ethyl 4-nitro-3-(*p*-tolyl)butanoate (4c). Intermediate **3c** was treated with nitromethane according to the general procedure for the synthesis of **4a**–**4d** to obtain the desired product **4c** as colorless oil in 90.7% yield. n_D^{20} 1.5196.

4.1.3.4. Ethyl 3-(3,5-dimethoxyphenyl)-4-nitrobutanoate (4d). Intermediate **3d** was treated with nitromethane according to the general procedure for the synthesis of **4a**–**4d** to obtain the desired product **4d** as yellow oil in 88.5% yield. n_D^{20} 1.5397.

4.1.4. General procedure for the preparation of target compounds (5a–5c, 6a–6b, 7a–7q and 8)

A mixture of ethyl 4-nitro-3-phenylbutanoate analogue (10 mmol), *p*-hydroxybenzaldehyde or vanillin (10 mmol), substituted benzylamine or 3-aminomethylpyridine (20 mmol), glacial acetic acid (2 mL) and anhydrous ethanol (50 mL) was stirred at reflux for about 24 h. After removal of the ethanol under vacuum, the residue washed with ethyl ether to afford the crude product, which was further added to 20 mL anhydrous ethanol, heated under reflux for 1 h and applied to suction filtration to obtain the desired products.

4.1.4.1. (±)-6-(4-Hydroxyphenyl)-5-nitro-4-phenyl-1-(pyridin-3-ylmethyl)piperidin-2-one (5a). Milk powder, yield: 43.9%, mp 250.3–250.7 °C. Purity: 99.1%, t_R = 3.37 min. IR (KBr) σ/cm^{-1} 3468, 1650, 1566, 1434, 1282. ^{1}H NMR (400 MHz, DMSO) δ 9.64 (s, 1H), 8.41 (d, J = 4.7 Hz, 1H), 8.15 (s, 1H), 7.42 (dd, J = 15.4, 7.6 Hz, 3H), 7.30 (dt, J = 19.4, 6.8 Hz, 4H), 7.09 (d, J = 8.4 Hz, 2H), 6.67 (d, J = 8.4 Hz, 2H), 5.66 (t, J = 10.8 Hz, 1H), 4.79 (d, J = 9.9 Hz, 1H), 4.70 (d, J = 15.5 Hz, 1H), 3.97–3.82 (m, 2H), 3.17 (dd, J = 16.9, 13.1 Hz, 1H), 2.72 (dd, J = 17.1, 4.8 Hz, 1H). ^{13}C NMR (100 MHz, DMSO) δ 168.66, 158.54, 149.30, 148.51, 138.49, 135.68, 133.04, 130.20, 129.14, 128.31, 128.00, 125.70, 123.72, 115.93, 92.94, 64.59, 44.97, 42.96, 38.01. ESI-MS [M−H]$^-$ (m/z):402.1. $C_{23}H_{21}N_3O_4$ [403.15].

4.1.4.2. (±)-4-(2-Chlorophenyl)-6-(4-hydroxyphenyl)-5-nitro-1-(pyridin-3-ylmethyl)piperidin-2-one (5b). Milk powder, yield: 44.8%, mp 231.4–233.8 °C. Purity: 96.2%, t_R = 4.32 min. IR (KBr) σ/cm^{-1} 3467, 1614, 1559, 1434, 1279. ^{1}H NMR (400 MHz, DMSO) δ 9.62 (s, 1H), 8.37 (d, J = 3.6 Hz, 1H), 8.11 (s, 1H), 7.78 (d, J = 7.5 Hz, 1H), 7.40 (dt, J = 17.3, 7.9 Hz, 3H), 7.26 (dd, J = 12.6, 7.8, 2.9 Hz, 2H), 7.12 (d, J = 8.4 Hz, 2H), 6.63 (d, J = 8.4 Hz, 2H), 5.93–5.76 (m, 1H), 4.92 (d, J = 9.8 Hz, 1H), 4.44 (dd, J = 17.0, 16.5, 10.2 Hz, 2H), 4.14 (d, J = 15.5 Hz, 1H), 3.04 (dd, J = 16.8, 13.0 Hz, 1H), 2.74 (dd, J = 17.1, 5.1 Hz, 1H). ^{13}C NMR (100 MHz, DMSO) δ 168.27, 158.57, 149.25, 148.37, 135.63, 133.35, 133.21, 130.44, 130.22, 129.91, 128.32, 125.40, 123.59, 115.82, 91.29, 64.82, 45.58. ESI-MS [M−H]$^-$ (m/z):436.1. $C_{23}H_{20}ClN_3O_4$ [437.11].

4.1.4.3. (±)-4-(3,5-Dimethoxyphenyl)-6-(4-hydroxyphenyl)-5-nitro-1-(pyridin-3-yl methyl)piperidin-2-one (5c). Milk powder, yield: 45.1%, mp 265.3–266.7 °C. Purity: 96.5%, t_R = 3.49 min. IR (KBr) σ/cm^{-1} 3467, 1643, 1556, 1396, 1285. ^{1}H NMR (400 MHz, DMSO) δ 9.63 (s, 1H), 8.41 (dd, J = 4.8, 1.5 Hz, 1H), 8.15 (d, J = 1.8 Hz, 1H), 7.43 (d, J = 7.9 Hz, 1H), 7.27 (dd, J = 7.8, 4.8 Hz, 1H), 7.08 (d, J = 8.5 Hz, 2H), 6.67 (d, J = 8.6 Hz, 2H), 6.58 (d, J = 2.2 Hz, 2H), 6.38 (t, J = 2.2 Hz, 1H), 5.65 (dd, J = 11.5, 10.0 Hz, 1H), 4.76 (d, J = 9.8 Hz, 1H), 4.71 (d, J = 15.5 Hz, 1H), 3.91 (d, J = 15.5 Hz, 1H), 3.81 (td, J = 12.5, 4.7 Hz, 1H), 3.71 (s, 6H), 3.14 (dd, J = 17.0, 13.0 Hz, 1H), 2.70 (dd, J = 17.1, 4.9 Hz, 1H). ^{13}C NMR (100 MHz, DMSO) δ 168.64, 161.02, 158.55, 149.29, 148.52, 140.78, 135.67, 133.03, 130.16, 125.71, 123.72, 115.95, 106.22, 99.66, 92.66, 64.61, 55.66, 43.06, 37.95. ESI-MS [M−H]$^-$ (m/z):462.1. $C_{25}H_{25}N_3O_6$ [463.17].

4.1.4.4. (±)-Methyl-4-((2-(4-hydroxyphenyl)-3-nitro-6-oxo-4-phenylpiperidin-1-yl)methyl)benzoate (6a). White powder, yield: 47.1%, mp 247.9–250.7 °C. Purity: 97.8%, t_R = 6.66 min. IR (KBr) σ/cm^{-1} 3468, 1727, 1612, 1558, 1436, 1281. ^{1}H NMR (400 MHz, DMSO) δ 9.64 (s, 1H), 7.86 (d, J = 7.9 Hz, 2H), 7.42 (d, J = 7.1 Hz, 2H), 7.32 (t, J = 7.2 Hz, 2H), 7.26 (d, J = 7.1 Hz, 1H), 7.17 (d, J = 7.8 Hz, 2H), 7.07 (d, J = 8.1 Hz, 2H), 6.68 (d, J = 8.1 Hz, 2H), 5.67 (t, J = 10.7 Hz, 1H), 4.91 (d, J = 15.7 Hz, 1H), 4.75 (d, J = 9.8 Hz, 1H), 4.02–3.65 (m, 5H), 3.29–3.10 (m, 1H), 2.76 (dd, J = 16.9, 4.2 Hz, 1H). ^{13}C NMR (100 MHz, DMSO) δ 168.58, 166.53, 158.56, 142.96, 138.44, 130.13, 129.60, 129.15, 128.70, 128.34, 128.16, 128.00, 125.70, 115.99, 93.05, 64.51, 52.51, 46.77, 43.03, 38.02. ESI-MS [M−H]$^-$ (m/z):459.1. $C_{26}H_{24}N_2O_6$ [460.16].

4.1.4.5. (±)-Methyl-4-((4-(2-chlorophenyl)-2-(4-hydroxyphenyl)-3-nitro-6-oxopiperidin-1-yl)methyl)benzoate (6b). White powder, yield: 42.6%, mp 240.3–241.3 °C. Purity: 97.9%, t_R = 7.32 min. IR (KBr) σ/cm^{-1} 3440, 3182, 1713, 1613, 1561, 1456, 1266. ^{1}H NMR (400 MHz, DMSO) δ 9.71 (s, 1H), 7.86 (t, J = 9.5 Hz, 3H), 7.48 (dd, J = 8.0, 1.0 Hz, 1H), 7.44 (t, J = 7.6 Hz, 1H), 7.37–7.31 (m, 1H), 7.16 (dd, J = 13.0, 8.4 Hz, 4H), 6.70 (d, J = 8.5 Hz, 2H), 5.92 (dd, J = 11.4, 10.1 Hz, 1H), 4.90 (d, J = 9.8 Hz, 1H), 4.76 (d, J = 15.7 Hz, 1H), 4.46 (td, J = 12.4, 5.0 Hz, 1H), 4.08 (d, J = 15.7 Hz, 1H), 3.88 (s, 3H), 3.13 (dd, J = 16.9, 13.1 Hz, 1H), 2.81 (dd, J = 17.1, 5.0 Hz, 1H). ^{13}C NMR (100 MHz, DMSO) δ 168.17, 166.52, 158.61, 143.24, 135.65, 133.20, 130.34, 130.22, 129.48, 128.59, 128.31, 128.13, 125.33, 115.87, 91.33, 64.72, 52.50, 47.31, 37.36. ESI-MS [M−H]$^-$ (m/z):493.1. $C_{26}H_{23}ClN_2O_6$ [494.12].

4.1.4.6. (±)-1-Benzyl-6-(4-hydroxyphenyl)-5-nitro-4-phenylpiperidin-2-one (7a). White powder, yield: 34.5%, mp 251.0–253.3 °C. Purity: 97.1%, t_R = 6.04 min. IR (KBr) σ/cm^{-1} 3463, 1614,

1557, 1495, 1276. ^{1}H NMR (400 MHz, DMSO) δ 9.64 (s, 1H), 7.41 (d, J = 7.3 Hz, 2H), 7.29 (dt, J = 12.7, 7.0 Hz, 6H), 7.10–6.97 (m, 4H), 6.72 (d, J = 8.4 Hz, 2H), 5.72–5.56 (m, 1H), 5.05 (d, J = 15.2 Hz, 1H), 4.67 (d, J = 9.9 Hz, 1H), 3.90–3.73 (m, 1H), 3.53 (d, J = 15.2 Hz, 1H), 3.17 (dd, J = 17.0, 13.3 Hz, 1H), 2.81–2.69 (m, 1H). ^{13}C NMR (100 MHz, DMSO) δ 168.35, 158.50, 138.42, 136.95, 129.93, 129.36, 129.11, 128.85, 128.63, 128.31, 128.00, 127.50, 125.99, 116.06, 93.31, 64.06, 46.34, 43.00, 38.00. ESI-MS $[M-H]^-$ (m/z):401.1. $C_{24}H_{22}N_2O_4$ [402.16].

4.1.4.7. (±)-1-(4-Fluorobenzyl)-6-(4-hydroxyphenyl)-5-nitro-4-phenylpiperidin-2-one (7b). White foam, yield: 26.7%, mp 269.1–271.0 °C. Purity: 96.7%, t_R = 10.77 min. IR (KBr) σ/cm^{-1} 3448, 2923, 1613, 1558, 1459, 1245. ^{1}H NMR (400 MHz, DMSO) δ 9.70 (s, 1H), 7.45 (d, J = 7.3 Hz, 2H), 7.37 (t, J = 7.4 Hz, 2H), 7.30 (t, J = 7.2 Hz, 1H), 7.18–7.07 (m, 6H), 6.75 (d, J = 8.5 Hz, 2H), 5.73–5.63 (m, 1H), 4.95 (d, J = 15.1 Hz, 1H), 4.74 (d, J = 9.8 Hz, 1H), 3.86 (td, J = 12.5, 4.7 Hz, 1H), 3.70 (d, J = 15.2 Hz, 1H), 3.21 (dd, J = 17.0, 13.2 Hz, 1H), 2.77 (dd, J = 17.0, 4.8 Hz, 1H). ^{13}C NMR (100 MHz, DMSO) δ 168.44, 160.46, 158.51, 138.42, 133.33, 133.30, 130.09, 130.02, 129.13, 128.32, 128.00, 125.87, 116.00, 115.61, 115.40, 93.19, 64.18, 45.92, 42.97, 38.00. ESI-MS $[M-H]^-$ (m/z):419.1. $C_{24}H_{21}FN_2O_4$ [420.15].

4.1.4.8. (±)-6-(4-Hydroxyphenyl)-1-(4-methylbenzyl)-5-nitro-4-phenylpiperidin-2-one (7c). White powder, yield: 37.2%, mp 275.6–278.1 °C. Purity: 95.4%, t_R = 8.95 min. IR (KBr) σ/cm^{-1} 3449, 3125, 1617, 1561, 1456, 1273. ^{1}H NMR (400 MHz, DMSO) δ 9.70 (s, 1H), 7.42 (d, J = 7.3 Hz, 2H), 7.33 (t, J = 7.4 Hz, 2H), 7.27 (d, J = 7.2 Hz, 1H), 7.13 (d, J = 7.8 Hz, 2H), 7.06 (d, J = 8.4 Hz, 2H), 6.94 (d, J = 7.9 Hz, 2H), 6.76 (d, J = 8.5 Hz, 2H), 5.63 (dd, J = 11.5, 10.1 Hz, 1H), 5.12 (d, J = 15.0 Hz, 1H), 4.63 (d, J = 9.9 Hz, 1H), 3.77 (td, J = 12.6, 4.6 Hz, 1H), 3.40 (d, J = 15.1 Hz, 1H), 3.18 (dd, J = 16.9, 13.2 Hz, 1H), 2.75 (dd, J = 17.0, 4.7 Hz, 1H), 2.30 (s, 3H). ^{13}C NMR (100 MHz, DMSO) δ 168.27, 158.50, 138.38, 136.68, 133.77, 129.88, 129.50, 129.11, 128.32, 128.09, 128.02, 126.05, 116.10, 93.37, 63.82, 45.83, 42.98, 37.98, 21.17. ESI-MS $[M-H]^-$ (m/z):415.1. $C_{25}H_{24}N_2O_4$ [416.17].

4.1.4.9. (±)-6-(4-Hydroxyphenyl)-1-(4-methoxybenzyl)-5-nitro-4-phenylpiperidin-2-one (7d). White powder, yield: 38.6%, mp 277.9–279.1 °C. Purity: 96.1%, t_R = 8.5 min. IR (KBr) σ/cm^{-1} 3450, 3125, 1614, 1560, 1439, 1247. ^{1}H NMR (400 MHz, DMSO) δ 9.69 (s, 1H), 7.41 (d, J = 8.1 Hz, 2H), 7.32 (t, J = 7.4 Hz, 2H), 7.27 (d, J = 7.2 Hz, 1H), 7.07 (d, J = 8.4 Hz, 2H), 6.97 (d, J = 8.5 Hz, 2H), 6.87 (d, J = 8.6 Hz, 2H), 6.76 (d, J = 8.5 Hz, 2H), 5.61 (t, J = 10.8 Hz, 1H), 5.08 (d, J = 14.9 Hz, 1H), 4.64 (d, J = 9.8 Hz, 1H), 3.79–3.71 (m, 4H), 3.41 (d, J = 14.9 Hz, 1H), 3.17 (dd, J = 16.8, 13.3 Hz, 1H), 2.73 (dd, J = 17.0, 4.7 Hz, 1H). ^{13}C NMR (100 MHz, DMSO) δ 168.25, 158.82, 158.49, 138.38, 129.89, 129.52, 129.11, 128.72, 128.31, 128.01, 126.11, 116.09, 114.29, 93.42, 63.77, 55.47, 45.53, 42.99, 37.99. ESI-MS $[M-H]^-$ (m/z):431.1. $C_{25}H_{24}N_2O_5$ [432.17].

4.1.4.10. (±)-6-(4-Hydroxyphenyl)-1-(3-methoxybenzyl)-5-nitro-4-phenylpiperidin-2-one (7e). White powder, yield: 41.4%, mp 262.2–263.2 °C. Purity: 97.7%, t_R = 9.22 min. IR (KBr) σ/cm^{-1} 3467, 1618, 1560, 1452, 1278. ^{1}H NMR (400 MHz,) δ 9.67 (s), 7.41 (d, J = 7.2 Hz), 7.32 (t, J = 7.4 Hz), 7.28–7.19 (m), 7.06 (d, J = 8.5 Hz), 6.82 (dd, J = 8.1, 2.3 Hz), 6.72 (d, J = 8.5 Hz), 6.63 (d, J = 7.6 Hz), 6.52 (s), 5.63 (dd, J = 11.6, 10.0 Hz), 5.00 (d, J = 15.2 Hz), 4.68 (d, J = 9.9 Hz), 3.79 (td, J = 12.6, 4.7 Hz), 3.71 (s), 3.52 (d, J = 15.2 Hz), 3.16 (dd, J = 17.0, 13.2 Hz), 2.74 (dd, J = 17.1, 4.8 Hz). ^{13}C NMR (100 MHz, DMSO) δ 168.35, 159.69, 158.51, 138.61, 130.00, 129.11, 128.32, 128.03, 125.98, 120.12, 116.01, 113.75, 112.93, 93.27, 64.10, 55.37, 43.03. ESI-MS $[M-H]^-$ (m/z):431.1. $C_{25}H_{24}N_2O_5$ [432.17].

4.1.4.11. (±)-1-(3,4-Dimethoxybenzyl)-6-(4-hydroxyphenyl)-5-nitro-4-phenylpiperidin-2-one (7f). White powder, yield: 43.5%, mp 275.3–277.6 °C. Purity: 94.4%, t_R = 5.41 min. IR (KBr) σ/cm^{-1} 3467, 2961, 1610, 1560, 1450, 1271. ^{1}H NMR (400 MHz, DMSO) δ 9.70 (s, 1H), 7.44 (d, J = 7.1 Hz, 2H), 7.36 (t, J = 7.3 Hz, 2H), 7.30 (t, J = 7.2 Hz, 1H), 7.11 (d, J = 8.5 Hz, 2H), 6.93 (d, J = 8.3 Hz, 1H), 6.79 (d, J = 8.5 Hz, 2H), 6.65 (dd, J = 8.2, 1.7 Hz, 1H), 6.55 (d, J = 1.8 Hz, 1H), 5.63 (dd, J = 11.6, 9.9 Hz, 1H), 5.08 (d, J = 14.8 Hz, 1H), 4.69 (d, J = 9.8 Hz, 1H), 3.90–3.61 (m, 7H), 3.48 (d, J = 14.8 Hz, 1H), 3.20 (dd, J = 16.9, 13.2 Hz, 1H), 2.77 (dd, J = 17.0, 4.7 Hz, 1H). ^{13}C NMR (100 MHz, DMSO) δ 168.30, 158.49, 149.00, 148.42, 138.38, 129.99, 129.29, 129.10, 128.31, 128.01, 126.18, 120.53, 116.03, 112.33, 112.23, 93.48, 63.84, 55.96, 55.83, 45.98, 43.04, 37.96. ESI-MS $[M-H]^-$ (m/z):461.1. $C_{26}H_{26}N_2O_6$ [462.18].

4.1.4.12. (±)-1-Benzyl-4-(2-chlorophenyl)-6-(4-hydroxyphenyl)-5-nitropiperidin-2-one (7g). White powder, yield: 44.2%, mp 236.1–237.5 °C. Purity: 96.9%, t_R = 10.88 min. IR (KBr) σ/cm^{-1} 3468, 1618, 1561, 1453, 1271. ^{1}H NMR (400 MHz, DMSO) δ 9.65 (s, 1H), 7.78 (d, J = 7.7 Hz, 1H), 7.43 (d, J = 8.0 Hz, 1H), 7.38 (t, J = 7.5 Hz, 1H), 7.32–7.21 (m, 4H), 7.08 (d, J = 8.4 Hz, 2H), 7.00 (d, J = 7.1 Hz, 2H), 6.70 (d, J = 8.4 Hz, 2H), 5.87–5.76 (m, 1H), 4.90 (d, J = 15.2 Hz, 1H), 4.75 (d, J = 9.8 Hz, 1H), 4.32 (td, J = 12.4, 4.9 Hz, 1H), 3.70 (d, J = 15.2 Hz, 1H), 3.06 (dd, J = 16.8, 13.2 Hz, 1H), 2.76 (dd, J = 17.1, 4.9 Hz, 1H). ^{13}C NMR (100 MHz, DMSO) δ 167.92, 158.55, 137.20, 135.53, 133.17, 130.23, 130.13, 129.94, 128.78, 128.31, 127.99, 127.48, 125.66, 115.99, 91.62, 64.30, 46.82, 37.30. ESI-MS $[M-H]^-$ (m/z):435.1. $C_{24}H_{21}ClN_2O_4$ [436.12].

4.1.4.13. (±)-4-(2-Chlorophenyl)-6-(4-hydroxyphenyl)-1-(4-methylbenzyl)-5-nitropiperidin-2-one (7h). White powder, yield: 48.6%, mp 265.6–266.3 °C. Purity: 99.3%, t_R = 12.97 min. IR (KBr) σ/cm^{-1} 3224, 1619, 1558, 1460, 1271. ^{1}H NMR (400 MHz, DMSO) δ 9.67 (s, 1H), 7.77 (d, J = 7.6 Hz, 1H), 7.42 (d, J = 7.9 Hz, 1H), 7.37 (t, J = 7.5 Hz, 1H), 7.28 (t, J = 7.6 Hz, 1H), 7.09 (t, J = 7.7 Hz, 4H), 6.90 (d, J = 7.8 Hz, 2H), 6.74 (d, J = 8.4 Hz, 2H), 5.87–5.73 (m, 1H), 4.98 (d, J = 15.0 Hz, 1H), 4.68 (d, J = 9.7 Hz, 1H), 4.28 (td, J = 12.4, 4.8 Hz, 1H), 3.53 (d, J = 15.0 Hz, 1H), 3.06 (dd, J = 16.8, 13.3 Hz, 1H), 2.75 (dd, J = 17.1, 4.9 Hz, 1H), 2.27 (s, 3H). ^{13}C NMR (100 MHz, DMSO) δ 167.82, 158.57, 136.69, 135.47, 133.98, 133.16, 130.22, 130.04, 129.93, 129.45, 128.30, 128.09, 125.76, 116.07, 91.73, 64.06, 46.26, 37.29, 21.15. ESI-MS $[M-H]^-$ (m/z):449.1. $C_{25}H_{23}ClN_2O_4$ [450.13].

4.1.4.14. (±)-4-(2-Chlorophenyl)-6-(4-hydroxyphenyl)-1-(4-methoxybenzyl)-5-nitropiperidin-2-one (7i). White powder, yield: 42.4%, mp 268.0–269.7 °C. Purity: 98.6%, t_R = 8.57 min. IR (KBr) σ/cm^{-1} 3436, 3199, 1618, 1557, 1462, 1272. ^{1}H NMR (400 MHz, DMSO) δ 9.67 (s, 1H), 7.76 (d, J = 7.7 Hz, 1H), 7.42 (d, J = 8.0 Hz, 1H), 7.37 (t, J = 7.4 Hz, 1H), 7.28 (t, J = 7.5 Hz, 1H), 7.08 (d, J = 8.4 Hz, 2H), 6.93 (d, J = 8.5 Hz, 2H), 6.84 (d, J = 8.6 Hz, 2H), 6.74 (d, J = 8.4 Hz, 2H), 5.85–5.73 (m, 1H), 4.94 (d, J = 14.9 Hz, 1H), 4.69 (d, J = 9.7 Hz, 1H), 4.26 (td, J = 12.4, 4.8 Hz, 1H), 3.74 (d, J = 9.2 Hz, 3H), 3.53 (d, J = 14.8 Hz, 1H), 3.04 (dd, J = 16.8, 13.3 Hz, 1H), 2.74 (dd, J = 17.1, 4.9 Hz, 1H). ^{13}C NMR (100 MHz, DMSO) δ 167.79, 158.82, 158.55, 135.47, 133.16, 130.22, 130.05, 129.93, 129.52, 128.94, 128.30, 125.81, 116.05, 114.26, 91.76, 64.00, 55.47, 45.95, 38.96, 37.31. ESI-MS $[M-H]^-$ (m/z):465.1. $C_{25}H_{23}ClN_2O_5$ [466.13].

4.1.4.15. (±)-4-(2-Chlorophenyl)-6-(4-hydroxyphenyl)-1-(3-methoxybenzyl)-5-nitropiperidin-2-one (7j). White powder, yield: 38.8%, mp 228.8–230.4 °C. Purity: 93.9%, t_R = 9.89 min. IR (KBr) σ/cm^{-1} 3468, 1613, 1560, 1487, 1276. ^{1}H NMR (400 MHz, DMSO) δ 9.65 (s, 1H), 7.77 (d, J = 7.6 Hz, 1H), 7.43 (d,

J = 7.9 Hz, 1H), 7.38 (t, J = 7.3 Hz, 1H), 7.29 (t, J = 7.6 Hz, 1H), 7.20 (t, J = 7.9 Hz, 1H), 7.08 (d, J = 8.4 Hz, 2H), 6.79 (dd, J = 8.2, 2.0 Hz, 1H), 6.70 (d, J = 8.4 Hz, 2H), 6.61 (d, J = 7.5 Hz, 1H), 6.50 (s, 1H), 5.87–5.74 (m, 1H), 4.86 (d, J = 15.3 Hz, 1H), 4.75 (d, J = 9.7 Hz, 1H), 4.32 (td, J = 12.4, 4.8 Hz, 1H), 3.68 (d, J = 15.5 Hz, 4H), 3.06 (dd, J = 16.9, 13.2 Hz, 1H), 2.75 (dd, J = 17.1, 4.9 Hz, 1H). ^{13}C NMR (100 MHz, DMSO) δ 167.93, 159.66, 158.57, 138.80, 135.50, 133.16, 130.23, 130.15, 129.95, 129.90, 128.31, 125.73, 120.12, 115.96, 113.53, 113.01, 91.62, 64.34, 55.35, 46.80, 37.25. ESI-MS $[M-H]^-$ (m/z):465.1. $C_{25}H_{23}ClN_2O_5$ [466.13].

4.1.4.16. (±)-1-Benzyl-6-(4-hydroxyphenyl)-5-nitro-4-(*p*-tolyl) piperidin-2-one (7k). White powder, yield: 37.7%, mp 263.2–264.8 °C. Purity: 96.8%, t_R = 9.5 min. IR (KBr) σ/cm^{-1} 3436, 3227, 1629, 1561, 1448, 1276. ^{1}H NMR (400 MHz, DMSO) δ 9.64 (s, 1H), 7.31–7.22 (m, 5H), 7.11 (d, J = 7.9 Hz, 2H), 7.06–7.01 (m, 4H), 6.72 (d, J = 8.4 Hz, 2H), 5.58 (dd, J = 11.3, 10.2 Hz, 1H), 5.06 (d, J = 15.3 Hz, 1H), 4.66 (d, J = 9.8 Hz, 1H), 3.74 (td, J = 12.6, 4.6 Hz, 1H), 3.53 (d, J = 15.2 Hz, 1H), 3.15 (dd, J = 16.9, 13.2 Hz, 1H), 2.71 (dd, J = 17.1, 4.7 Hz, 1H), 2.23 (s, 3H). ^{13}C NMR (100 MHz, DMSO) δ 168.43, 158.50, 137.54, 136.96, 135.38, 129.91, 129.67, 128.85, 128.00, 127.87, 127.50, 126.06, 116.06, 93.46, 64.06, 46.33, 42.67, 38.06, 21.08. ESI-MS $[M-H]^-$ (m/z):415.1. $C_{25}H_{24}N_2O_4$ [416.17].

4.1.4.17. (±)-6-(4-Hydroxyphenyl)-1-(4-methylbenzyl)-5-nitro-4-(*p*-tolyl)piperidin-2-one (7l). White powder, yield: 38.1%, mp 265.2–266.7 °C. Purity: 95.2%, t_R = 14.49 min. IR (KBr) σ/cm^{-1} 3436, 3130, 1613, 1562, 1447, 1280. ^{1}H NMR (400 MHz, DMSO) δ 9.63 (s, 1H), 7.25 (d, J = 7.9 Hz, 2H), 7.09 (d, J = 7.5 Hz, 4H), 7.01 (d, J = 8.3 Hz, 2H), 6.90 (d, J = 7.7 Hz, 2H), 6.71 (d, J = 8.4 Hz, 2H), 5.53 (t, J = 10.8 Hz, 1H), 5.07 (d, J = 15.0 Hz, 1H), 4.58 (d, J = 9.9 Hz, 1H), 3.67 (td, J = 12.6, 4.5 Hz, 1H), 3.36 (d, J = 15.1 Hz, 1H), 3.11 (dd, J = 16.8, 13.4 Hz, 1H), 2.67 (dd, J = 17.0, 4.6 Hz, 1H), 2.26 (s, 3H), 2.21 (s, 3H). ^{13}C NMR (100 MHz, DMSO) δ 168.34, 158.48, 137.53, 136.67, 135.34, 133.79, 129.85, 129.66, 129.49, 128.08, 127.86, 126.14, 116.09, 93.54, 63.82, 45.83, 42.65, 38.05, 21.16, 21.07. ESI-MS $[M-H]^-$ (m/z):429.1. $C_{26}H_{26}N_2O_4$ [430.19].

4.1.4.18. (±)-6-(4-Hydroxyphenyl)-1-(4-methoxybenzyl)-5-nitro-4-(*p*-tolyl)piperidin-2-one (7m). White powder, yield: 39.6%, mp 259.9–262.2 °C. Purity: 96.1%, t_R = 7.39 min. IR (KBr) σ/cm^{-1} 3467, 2960, 1613, 1560, 1437, 1243. ^{1}H NMR (400 MHz, DMSO) δ 9.66 (s, 1H), 7.27 (d, J = 8.0 Hz, 2H), 7.07 (dd, J = 24.5, 8.2 Hz, 4H), 6.95 (d, J = 8.5 Hz, 2H), 6.85 (d, J = 8.6 Hz, 2H), 6.74 (d, J = 8.4 Hz, 2H), 5.55 (dd, J = 11.4, 10.2 Hz, 1H), 5.06 (d, J = 14.9 Hz, 1H), 4.60 (d, J = 9.8 Hz, 1H), 3.75–3.63 (m, 4H), 3.38 (d, J = 14.9 Hz, 1H), 3.13 (dd, J = 16.9, 13.2 Hz, 1H), 2.68 (dd, J = 17.0, 4.7 Hz, 1H), 2.23 (s, 3H). ^{13}C NMR (100 MHz, DMSO) δ 168.32, 158.82, 158.47, 137.53, 135.34, 129.85, 129.66, 129.51, 128.74, 127.85, 126.19, 116.09, 114.29, 93.58, 63.77, 55.48, 45.52, 42.66, 38.06, 21.07. ESI-MS $[M-H]^-$ (m/z):445.1. $C_{26}H_{26}N_2O_5$ [446.18].

4.1.4.19. (±)-6-(4-Hydroxyphenyl)-1-(3-methoxybenzyl)-5-nitro-4-(*p*-tolyl)piperidin-2-one (7n). White powder, yield: 44.6%, mp 250.2–253.6 °C. Purity: 96.5%, t_R = 8.34 min. IR (KBr) σ/cm^{-1} 3436, 1614, 1561, 1434, 1278. ^{1}H NMR (400 MHz, DMSO) δ 9.67 (s, 1H), 7.29 (d, J = 7.8 Hz, 2H), 7.21 (d, J = 8.0 Hz, 1H), 7.12 (d, J = 7.8 Hz, 2H), 7.06 (d, J = 8.2 Hz, 2H), 6.82 (d, J = 8.2 Hz, 1H), 6.72 (d, J = 8.2 Hz, 2H), 6.63 (d, J = 7.5 Hz, 1H), 6.53 (s, 1H), 5.59 (t, J = 10.8 Hz, 1H), 5.00 (d, J = 15.2 Hz, 1H), 4.67 (d, J = 9.8 Hz, 1H), 3.80–3.64 (m, 4H), 3.52 (d, J = 15.2 Hz, 1H), 3.15 (dd, J = 16.7, 13.4 Hz, 1H), 2.71 (dd, J = 17.0, 4.5 Hz, 1H), 2.24 (s, 3H). ^{13}C NMR (100 MHz, DMSO) δ 168.42, 159.70, 158.50, 138.62, 137.54, 135.36, 129.97, 129.93, 129.66, 127.88, 126.05, 120.13, 116.01, 113.74, 112.94, 93.43, 64.09, 55.37, 46.32, 42.70, 38.01, 21.08. ESI-MS $[M-H]^-$ (m/z):445.1. $C_{26}H_{26}N_2O_5$ [446.18].

4.1.4.20. (±)-1-Benzyl-4-(3,5-dimethoxyphenyl)-6-(4-hydroxyphenyl)-5-nitropiperidin-2-one (7o). White powder, yield: 40.9%, mp 263.0–264.9 °C. Purity: 96.3%, t_R = 8.13 min. IR (KBr) σ/cm^{-1} 3468, 2965, 1611, 1591, 1432, 1207. ^{1}H NMR (400 MHz, DMSO) δ 9.64 (s, 1H), 7.27 (dq, J = 14.2, 7.0 Hz, 3H), 7.02 (d, J = 8.2 Hz, 4H), 6.71 (d, J = 8.5 Hz, 2H), 6.59 (d, J = 2.1 Hz, 2H), 6.37 (s, 1H), 5.66–5.57 (m, 1H), 5.04 (d, J = 15.3 Hz, 1H), 4.63 (d, J = 9.8 Hz, 1H), 3.78–3.66 (m, 7H), 3.52 (d, J = 15.2 Hz, 1H), 3.14 (dd, J = 16.9, 13.2 Hz, 1H), 2.71 (dd, J = 17.1, 4.7 Hz, 1H). ^{13}C NMR (100 MHz, DMSO) δ 168.33, 161.01, 158.50, 140.72, 136.93, 129.90, 128.85, 127.98, 127.51, 125.98, 116.05, 106.23, 99.70, 92.96, 64.07, 55.66, 46.31, 43.07, 37.94. ESI-MS $[M-H]^-$ (m/z):461.1. $C_{26}H_{26}N_2O_6$ [462.18].

4.1.4.21. (±)-4-(3,5-Dimethoxyphenyl)-6-(4-hydroxyphenyl)-1-(3-methoxybenzyl)-5-nitropiperidin-2-one (7p). White powder, yield: 41.6%, mp 226.1–227.7 °C. Purity: 98.2%, t_R = 9.77 - min. IR (KBr) σ/cm^{-1} 3468, 1611, 1592, 1491, 1327. ^{1}H NMR (400 MHz, DMSO) δ 9.65 (s, 1H), 7.21 (t, J = 7.9 Hz, 1H), 7.04 (d, J = 8.4 Hz, 2H), 6.81 (dd, J = 8.2, 2.2 Hz, 1H), 6.72 (d, J = 8.4 Hz, 2H), 6.61 (dd, J = 12.2, 4.8 Hz, 3H), 6.51 (s, 1H), 6.38 (s, 1H), 5.67–5.54 (m, 1H), 4.99 (d, J = 15.2 Hz, 1H), 4.65 (d, J = 9.8 Hz, 1H), 3.77–3.71 (m, 1H), 3.70 (s, 9H), 3.51 (d, J = 15.2 Hz, 1H), 3.13 (dd, J = 17.0, 13.2 Hz, 1H), 2.71 (dd, J = 17.1, 4.7 Hz, 1H). ^{13}C NMR (100 MHz, DMSO) δ 168.33, 161.01, 159.70, 158.52, 140.71, 138.61, 129.97, 125.99, 120.13, 116.02, 113.81, 112.92, 106.25, 99.69, 92.97, 64.13, 63.88, 55.66, 55.37, 46.35, 43.12, 37.90. ESI-MS $[M-H]^-$ (m/z):491.1. $C_{27}H_{28}N_2O_7$ [492.19].

4.1.4.22. (±)-1-(3,4-Dimethoxybenzyl)-4-(3,5-dimethoxyphenyl)-6-(4-hydroxyphenyl)-5-nitropiperidin-2-one (7q). White powder, yield: 43.8%, mp 274.7–276.1 °C. Purity: 96.6%, t_R = 5.02 min. IR (KBr) σ/cm^{-1} 3468, 1623, 1595, 1434, 1256. ^{1}H NMR (400 MHz, DMSO) δ 9.66 (s, 1H), 7.05 (d, J = 8.5 Hz, 2H), 6.88 (d, J = 8.3 Hz, 1H), 6.75 (d, J = 8.6 Hz, 2H), 6.59 (dd, J = 9.7, 2.0 Hz, 3H), 6.49 (d, J = 1.9 Hz, 1H), 6.38 (t, J = 2.2 Hz, 1H), 5.58 (dd, J = 11.6, 9.9 Hz, 1H), 5.03 (d, J = 14.8 Hz, 1H), 4.61 (d, J = 9.8 Hz, 1H), 3.75–3.64 (m, 13H), 3.42 (d, J = 14.8 Hz, 1H), 3.13 (dd, J = 17.0, 13.1 Hz, 1H), 2.70 (dd, J = 17.0, 4.7 Hz, 1H). ^{13}C NMR (100 MHz, DMSO) δ 168.28, 161.00, 158.50, 148.99, 148.42, 140.68, 129.96, 129.28, 126.17, 120.53, 116.04, 112.36, 112.21, 106.26, 93.14, 63.85, 55.96, 55.82, 55.66, 45.96, 43.11. ESI-MS $[M-H]^-$ (m/z):521.0. $C_{28}H_{30}N_2O_8$ [522.20].

4.1.4.23. (±)-1-Benzyl-4-(2-chlorophenyl)-6-(4-hydroxy-3-methoxyphenyl)-5-nitropiperidin-2-one (8). Off-white powder, yield: 39%, mp 237.2–238.4 °C. Purity: 97.6%, t_R = 10.55 - min. IR (KBr) σ/cm^{-1} 3338, 1637, 1557, 1443, 1281. ^{1}H NMR (400 MHz, DMSO) δ 9.22 (s, 1H), 7.79 (d, J = 7.6 Hz, 1H), 7.45 (dd, J = 8.0, 1.0 Hz, 1H), 7.41 (t, J = 7.6 Hz, 1H), 7.34–7.20 (m, 4H), 7.02 (d, J = 6.9 Hz, 2H), 6.89 (d, J = 1.6 Hz, 1H), 6.68 (d, J = 8.0 Hz, 1H), 6.59 (dd, J = 8.0, 1.7 Hz, 1H), 5.88 (dd, J = 11.4, 10.0 Hz, 1H), 4.81 (d, J = 9.8 Hz, 1H), 4.74 (d, J = 15.3 Hz, 1H), 4.38 (td, J = 12.5, 5.0 Hz, 1H), 3.93 (d, J = 15.2 Hz, 1H), 3.65 (s, 3H), 3.06 (dd, J = 16.9, 13.1 Hz, 1H), 2.79 (dd, J = 17.1, 5.1 Hz, 1H). ^{13}C NMR (100 MHz, DMSO) δ 167.98, 148.29, 147.84, 137.63, 135.67, 133.19, 130.25, 129.94, 128.63, 128.33, 127.96, 127.31, 126.04, 122.13, 115.53, 112.21, 91.33, 64.97, 56.03, 47.31, 37.46. ESI-MS $[M-H]^-$ (m/z):465.1. $C_{25}H_{23}ClN_2O_5$ [466.13].

4.2. Molecular modeling studies

4.2.1. Pharmacophore mapping

Combined with the 3D crystal structure of MyD88, the action mechanism of MyD88 (dimerization) and the effect that acted on MyD88 by **ST2825** (a peptidomimetic inhibitor), we used the software Catalyst to generate the optimal pharmacophore model (Fig. 1). On the basis of the constructed pharmacophore model, we screened the library to find structures that matching this model. As a result, compounds with piperidone framework were chosen as a scaffold for further chemical modification. According to the Lipinski principle and other criteria used for design, twenty-three 2-piperidone derivatives were selected and their activities of MyD88 inhibition were predicted by pharmacophore. Moreover, the physicochemical properties were calculated using Pallas 3.3.2.6 software and mapping of designed compounds (the default structure: 4*R*,5*R*,6*S*) on the optimal pharmacophore developed against MyD88 showed in Table 1 and Figure 3, respectively.

4.2.2. Docking analysis

Molecular docking studies were performed using software package Ligandfit of Cerius2 (Accelrys Inc.). The crystal structure of MyD88 (PDB ID: 4DOM) was downloaded from Protein Data bank (PDB) database (shown in Fig. 4A). All the water molecules and inactive groups in PDB files were removed and hydrogen atoms were subsequently added to the protein. We used the compound **7q** (the default structure: 4*R*,5*R*,6*S*) to investigate the intermolecular interactions between the molecules and the protein. The Ligandfit docking protocol docked a ligand into the active site using a parallel algorithm or lattice distributed algorithm. During the docking process, the best ten poses of molecules were retained, evaluated and ranked using the scoring functions. Herein, LigScore2 and Jain were used as the scoring functions to estimate which of the conformations were best complements to the MyD88 active site.

4.3. Inhibition of self-mediated $A\beta_{1-42}$ aggregation

4.3.1. ThT assay

Inhibition of self-mediated $A\beta_{1-42}$ aggregation was gauged using a thioflavin T (ThT) fluorescence assay. $A\beta_{1-42}$ (purchased from Sigma–Aldrich Co. LLC.) was pretreated by 1,1,1,3,3,3-hexafluoro-2-propanal (HFIP) to a concentration of 1 mg/mL, sonicated in ultrasonic cleaning apparatus for 5 min, averaged into microcentrifuge tubes, dried under vacuum, and stored at −20 °C. The HFIP pretreated $A\beta_{1-42}$ was dissolved in dimethyl sulfoxide (DMSO) to a concentration of 200 μM as the stored solution. Meanwhile, each tested compound was prepared also in DMSO to a concentration of 200 μM prior to use. Amounts of 5 μL compound (200 μM) and 5 μL $A\beta_{1-42}$ (200 μM) were added into 40 μL of phosphate buffered saline (PBS at pH 7.4). The final concentration of each compound was 20 μM and was disposed in independent triplicates.

After incubation for 24 h at room temperature on thermostatic shaker, 100 μL of 5 μM ThT in 50 mM glycine–NaOH buffer (pH 8.5) was added to the reaction solution. Fluorescence was measured with excitation and emission wavelengths at 435 nm and 490 nm, respectively on a F-4600 fluorospectrophotometer (HITACHI, Tokyo, Japan).

4.3.2. AFM assay

The HFIP-treated $A\beta_{1-42}$ was dissolved in DMSO to give the 1 mM stock solution. $A\beta_{1-42}$ (0.5 mM, 5 μL) and PBS (pH 7.4, 90 μL) were incubated in the presence and absence of the compound **7q** (1 mM, 5 μL) for 4 days at 30 °C. The final concentration of $A\beta_{1-42}$ and **7q** were 25 μM and 50 μM, respectively. For imaging, aliquots of the incubating solution (10 μL) were taken out and deposited on the mica sheet directly. The deposited droplet was left on the mica sheet for 10 min. Then, the samples were gently rinsed with ultra-pure water to remove excess salts and dried with nitrogen. The morphology of the samples was obtained on a Pico-Scan SPM-9700 microscope (Shimadzu, Japan) with tapping mode.

4.4. Measurement of cytokines

The murine microglia cell line (BV-2) was obtained from the China Infrastructure of Cell Line Resources. The cells were maintained in complete DMEM-H medium supplemented with 10% fetal bovine serum (FBS) at 37 °C in a humidified 5% CO_2 atmosphere. BV-2 cells were plated in 96-well plate at a density of 1×10^4 cells/well and cultured for 24 h. To evaluate the cytotoxic effect of the designed compounds, the compound **7q** was selected at various concentrations (0.008, 0.04, 0.2, 1 and 5 μmol/L) with or without LPS and estimated using MTT [(3-(4,5-dimethylthiazol-2-yl)-(2,5-diphenyltetrazolium bromide] assay. Absorbance was measured using a microplate reader at a wavelength of 490 nm.

For cytokine immunoassays, BV-2 cells were seeded into 24-well plate (2×10^4 cells/well) and pre-treated with 0.0016, 0.008, 0.04, 0.2 and 1 μmol/L of compounds for 3 h and further cultured 12 h with LPS (1 μg/mL). Supernatants were collected and centrifuged at the allotted time. The pro-inflammation cytokines TNF-α, IL-1β and IL-6 productions were quantified by enzyme-linked immunosorbent assay (ELISA) according to the protocol supplied by corresponding ELISA-kit (Boster Bioengineering Corp Ltd, China), respectively.

4.5. Prevention of inflammation mediated toxicity in SH-SY5Y cells

The human neuroblastoma cells SH-SY5Y were acquired from the China Infrastructure of Cell Line Resources. Cells were cultured in Dulbecco's modified Eagle medium/Ham's F-12 medium (DMEM/F-12, Sigma–Aldrich) with 10% (v/v) FBS and incubated at 37 °C with 5% CO_2. In order to evaluate the cytotoxic effect of the designed molecules to SH-SY5Y, cells were plated in 96-well plates at a density of 1×10^4 cells/well and incubated for 24 h, followed by treatment with different concentration (0.04, 0.2, 1 and 5 μmol/L) of the compound **7q**. After incubation for 24 h, the MTT was added and continued to culture for another 4 h. Absorbance was measured using a microplate reader at a wavelength of 490 nm.

The microglial cells BV-2 were seeded into 24-well plate (2×10^4 cells/well) and pretreated with 0.2, 1 and 5 μM of compound **7q** for 3 h and stimulated with 1 μg/mL of LPS for 12 h. Then the supernatants were harvested, clarified by centrifugation to obtain the so called conditioned media (CM). Next, the SH-SY5Y cells were inoculated in 96-well plate (5×10^3 cells/well) for 24 h. After 24 h, cells were starved with serum-free media overnight before treated by the conditioned media from LPS-stimulated BV-2 cells. Cell viability was determined by MTT assay. Absorbance was measured using a microplate reader at a wavelength of 490 nm.

4.6. Co-IP assay

The plasmids were constructed and sequenced: pcDNA 3.1-(Flag-MyD88) expressing full-length sequences of flag-tagged MyD88, pcDNA 3.1-(HA-MyD88) for HA-tagged MyD88, pcDNA 3.1-(Flag-con) for flag-tagged control and pcDNA 3.1-(HA-con) for HA-tagged control. The human embryonic kidney cells HEK-293 were acquired from the China Infrastructure of Cell Line Resources. Cells were cultured in Dulbecco's modified Eagle

medium with 10% (v/v) FBS and incubated at 37 °C with 5% CO_2. HEK-293 cells were plated in 6-well plate at a density of 9×10^5 -cells/well and cultured for 24 h. Then, HEK293 cells were transfected with single or combined plasmids using Lipofectamine 2000 (Invitrogen), and followed by treatment with different concentration (10 and 40 μM) of the compound **7q** after seven hours.

HEK293 cells were collected 24 h after transfection, washed in ice-cold PBS, and lysed in RIPA buffer (Beyotime Biotech). Cell lysates were collected and precleared by incubation for 3 h with a mixture of protein A/G agarose beads (Beyotime Biotech) under constant shaking at 4 °C. The homogenates were centrifuged at 2500 rpm for 5 min at 4 °C. For Co-IP, anti-HA antibody (Beyotime Biotech) were preincubated overnight with a mixture of protein A/G agarose beads under constant shaking at 4 °C for 4 h. After incubation, the beads were washed in ice-cold PBS and centrifuged at 2500 rpm for 5 min at 4 °C. Then, the immunocomplexes captured by protein beads were eluted in SDS–PAGE sample buffer for western blot (WB) analysis.

Acknowledgement

This work was supported by Grants from the Key Project of Independent Innovation Research Fund of Huazhong University of Science and Technology (2014YGYL017) to Prof. Feng-Chao Jiang.

Supplementary data

Supplementary data associated with this article can be found, in the online version, at http://dx.doi.org/10.1016/j.bmc.2016.03.010. These data include MOL files and InChiKeys of the most important compounds described in this article.

References and notes

1. Palmer, A. M. *Trends Pharmacol. Sci.* **2011**, *32*, 141.
2. Hamley, I. W. *Chem. Rev.* **2012**, *112*, 5147.
3. Hardy, J. *Neuron* **2006**, *52*, 3.
4. Tuppo, E. E.; Arias, H. R. *Int. J. Biochem. Cell Biol.* **2005**, *37*, 289.
5. Citron, M. *Nat. Rev. Drug. Disc.* **2010**, *9*, 387.
6. Bartus, R. T.; Dean, R. L.; Beer, B.; Lippa, A. S. *Science* **1982**, 408.
7. Weninger, S. C.; Yankner, B. A. *Nat. Med.* **2001**, *7*, 527.
8. Schenk, D. *Nat. Rev. Neurosci.* **2002**, *3*, 824.
9. Rizzo, S.; Rivière, C.; Piazzi, L.; Bisi, A.; Gobbi, S.; Bartolini, M.; Andrisano, V.; Morroni, F.; Tarozzi, A.; Monti, J.; Rampa, A. *J. Med. Chem.* **2008**, *51*, 2883.
10. Schwarz, S.; Lucas, S. D.; Sommerwerk, S.; Csuk, R. *Bioorg. Med. Chem.* **2014**, *22*, 3370.
11. Jan, A.; Gokce, O.; Luthi-Carter, R.; Lashuel, H. A. *J. Biol. Chem.* **2008**, *283*, 28176.
12. Walsh, D. M.; Selkoe, D. J. *Neuron* **2004**, *44*, 181.
13. Estrada, L. D.; Soto, C. *Curr. Top. Med. Chem.* **2007**, *7*, 115.
14. Gao, H. M.; Hong, J. S. *Trends Immunol.* **2008**, *29*, 357.
15. Combs, C. K. *J. Neuroimmune Pharm.* **2009**, *4*, 380.
16. Cameron, B.; Landreth, G. E. *Neurobiol. Dis.* **2010**, *37*, 503.
17. Akiyama, H.; Arai, T.; Kondo, H.; Tanno, E.; Haga, C.; Ikeda, K. *Alzheimer Dis. Assoc. Disord.* **2000**, *14*, S47.
18. Liu, B. *J. Pharmacol. Exp. Ther.* **2003**, *304*, 1.
19. Block, M. L.; Hong, J. *Prog. Neurobiol.* **2005**, *76*, 77.
20. Akira, S.; Takeda, K.; Kaisho, T. *Nat. Immunol.* **2001**, *2*, 675.
21. Dean, J. M.; Wang, X.; Kaindl, A. M.; Gressens, P.; Fleiss, B.; Hagberg, H.; Mallard, C. *Brain Behav. Immun.* **2010**, *24*, 776.
22. Carty, M.; Bowie, A. G. *Biochem. Pharmacol.* **2011**, *81*, 825.
23. Salminen, A.; Ojala, J.; Kauppinen, A.; Kaarniranta, K.; Suuronen, T. *Prog. Neurobiol.* **2009**, *87*, 181.
24. Monsonego, A.; Weiner, H. L. *Science* **2003**, *302*, 834.
25. Hopkins, A. L. *Nat. Chem. Biol.* **2008**, *4*, 682.
26. Cavalli, A.; Bolognesi, M. L.; Minarini, A.; Rosini, M.; Tumiatti, V.; Recanatini, M.; Melchiorre, C. *J. Med. Chem.* **2008**, *51*, 347.
27. Rampa, A.; Belluti, F.; Gobbi, S.; Bisi, A. *Curr. Top. Med. Chem.* **2011**, *11*, 2716.
28. Huang, W.; Tang, L.; Shi, Y.; Huang, S.; Xu, L.; Sheng, R.; Wu, P.; Li, J.; Zhou, N.; Hu, Y. *Bioorg. Med. Chem.* **2011**, *19*, 7158.
29. Lefterov, I.; Bookout, A.; Wang, Z.; Staufenbiel, M.; Mangelsdorf, D.; Koldamova, R. *Mol. Neurodegener.* **2007**, *2*, 20.
30. Zhang, Y. H.; Mann, D.; Raymick, J.; Sarkar, S.; Paule, M. G.; Lahiri, D. K.; Dumas, M.; Bell-Cohen, A.; Schmued, L. C. *Curr. Alzheimer Res.* **2014**, *11*, 299.
31. Fantò, N.; Gallo, G.; Ciacci, A.; Semproni, M.; Vignola, D.; Quaglia, M.; Bombardi, V.; Mastroianni, D.; Zibella, M. P.; Basile, G.; Sassano, M.; Ruggiero, V.; De Santis, R.; Carminati, P. *J. Med. Chem.* **2008**, *51*, 1189.
32. Loiarro, M.; Sette, C.; Gallo, G.; Ciacci, A.; Fanto, N.; Mastroianni, D.; Carminati, P.; Ruggiero, V. *J. Biol. Chem.* **2005**, *280*, 15809.
33. Qadeer, G.; Rama, N. H.; Shahb, S. J. H. *ARKIVOC* **2007**, *XIV*, 12.
34. Gao, L.; Xu, W.; Xiao, G. *Adv. Mater. Res.* **2013**, *634*, 869.
35. Ono, N.; Kamimura, A.; Kaji, A. *Synthesis* **1984**, *3*, 226.
36. Bhagwatheeswaran, H.; Gaur, S. P.; Jain, P. C. *Synthesis* **1976**, *9*, 615.
37. Nara, S.; Tanaka, R.; Eishima, J.; Hara, M.; Takahashi, Y.; Otaki, S.; Foglesong, R. J.; Hughes, P. F.; Turkington, S.; Kanda, Y. *J. Med. Chem.* **2003**, *46*, 2467.
38. Lipinski, C. A. *J. Pharmacol. Toxicol. Methods* **2000**, *44*, 235.
39. Snyder, G. A.; Cirl, C.; Jiang, J.; Chen, K.; Waldhuber, A.; Smith, P.; Rommler, F.; Snyder, N.; Fresquez, T.; Durr, S.; Tjandra, N.; Miethke, T.; Xiao, T. S. *Proc. Natl. Acad. Sci. U.S.A.* **2013**, *110*, 6985.
40. Jiang, Z.; Georgel, P.; Li, C.; Choe, J.; Crozat, K.; Rutschmann, S.; Du, X.; Bigby, T.; Mudd, S.; Sovath, S.; Wilson, I. A.; Olson, A.; Beutler, B. *Proc. Natl. Acad. Sci. U.S. A.* **2006**, *103*, 10961.
41. Wang, Y.; Wang, F.; Yu, J.; Jiang, F.; Guan, X.; Wang, C.; Li, L.; Cao, H.; Li, M.; Chen, J. *Bioorg. Med. Chem.* **2012**, *20*, 6513.
42. Khurana, R.; Coleman, C.; Ionescu-Zanetti, C.; Carter, S. A.; Krishna, V.; Grover, R. K.; Roy, R.; Singh, S. *J. Struct. Biol.* **2005**, *151*, 229.
43. Biancalana, M.; Koide, S. *Biochim. Biophys. Acta (BBA)—Proteins Proteomics* **2010**, *1804*, 1405.
44. Legleiter, J. *Methods Mol. Biol.* **2011**, *670*, 57.
45. Lehnardt, S.; Massillon, L.; Follett, P.; Jensen, F. E.; Ratan, R.; Rosenberg, P. A.; Volpe, J. J.; Vartanian, T. *Proc. Natl. Acad. Sci. U.S.A.* **2003**, *100*, 8514.
46. Dalcanale, E.; Montanart, F. *J. Org. Chem.* **1986**, *51*, 567.
47. Szymanski, W.; Wu, B.; Weiner, B.; de Wildeman, S.; Feringa, B. L.; Janssen, D. B. *J. Org. Chem.* **2009**, *74*, 9152.
48. Fukuyama, T.; Arai, M.; Matsubara, H.; Ryu, L. *J. Org. Chem.* **2004**, *69*, 8105.
49. Peterson, J. R.; Russell, M. E.; SurJasasmlta, I. B. *J. Chem. Eng. Data* **1988**, *33*, 534.
50. Finley, K. T.; Call, D. R.; Sovocool, G. W.; Hayles, W. J. *Can. J. Chem.* **1967**, *45*, 571.